frontiers | Frontiers in Cellular and Infection Microbiology

TYPE Original Research
PUBLISHED 09 March 2023
DOI 10.3389/fcimb.2023.1144210

OPEN ACCESS

EDITED BY
Elena G. Salina,
Research Center of Biotechnology of the Russian Academy of Sciences, Russia

REVIEWED BY
Martin I. Voskuil,
University of Colorado Denver, United States
Brian Weinrick,
Trudeau Institute, United States

*CORRESPONDENCE
Kyle H. Rohde
Kyle.rohde@ucf.edu

SPECIALTY SECTION
This article was submitted to Bacteria and Host, a section of the journal Frontiers in Cellular and Infection Microbiology

RECEIVED 13 January 2023
ACCEPTED 15 February 2023
PUBLISHED 09 March 2023

CITATION
Simcox BS, Tomlinson BR, Shaw LN and Rohde KH (2023) *Mycobacterium abscessus* DosRS two-component system controls a species-specific regulon required for adaptation to hypoxia. *Front. Cell. Infect. Microbiol.* 13:1144210. doi: 10.3389/fcimb.2023.1144210

Mycobacterium abscessus DosRS two-component system controls a species-specific regulon required for adaptation to hypoxia

Breven S. Simcox[1], Brooke R. Tomlinson[2], Lindsey N. Shaw[2] and Kyle H. Rohde[1]*

[1]Division of Immunology and Pathogenesis, Burnett School of Biomedical Sciences, College of Medicine, University of Central Florida, Orlando, FL, United States, [2]Department of Cell Biology, Microbiology and Molecular Biology, University of South Florida, Tampa, FL, United States

Mycobacterium abscessus (*Mab*), an emerging opportunistic pathogen, predominantly infects individuals with underlying pulmonary diseases such as cystic fibrosis (CF). Current treatment outcomes for *Mab* infections are poor due to *Mab's* inherent antibiotic resistance and unique host interactions that promote phenotypic tolerance and hinder drug access. The hypoxic, mucus-laden airways in the CF lung and antimicrobial phagosome within macrophages represent hostile niches *Mab* must overcome *via* alterations in gene expression for survival. Regulatory mechanisms important for the adaptation and long-term persistence of *Mab* within the host are poorly understood, warranting further genetic and transcriptomics study of this emerging pathogen. DosRS$_{Mab}$, a two-component signaling system (TCS), is one proposed mechanism utilized to subvert host defenses and counteract environmental stress such as hypoxia. The homologous TCS of *Mycobacterium tuberculosis* (*Mtb*), DosRS$_{Mtb}$, is known to induce a ~50 gene regulon in response to hypoxia, carbon monoxide (CO) and nitric oxide (NO) *in vitro* and *in vivo*. Previously, a small DosR$_{Mab}$ regulon was predicted using bioinformatics based on DosR$_{Mtb}$ motifs however, the role and regulon of DosRS$_{Mab}$ in *Mab* pathogenesis have yet to be characterized in depth. To address this knowledge gap, our lab generated a *Mab dosRS* knockout strain (*Mab*$_{\Delta dosRS}$) to investigate differential gene expression, and phenotype in an *in vitro* hypoxia model of dormancy. qRT-PCR and lux reporter assays demonstrate *Mab_dosR* and 6 predicted downstream genes are induced in hypoxia. In addition, RNAseq revealed induction of a much larger hypoxia response comprised of >1000 genes, including 127 differentially expressed genes in a *dosRS* mutant strain. Deletion of DosRS$_{Mab}$ led to attenuated growth under low oxygen conditions, a shift in morphotype from smooth to rough, and down-regulation of 216 genes. This study provides the first look at the global transcriptomic response of *Mab* to low oxygen conditions encountered in the airways of CF patients and within macrophage phagosomes. Our data also demonstrate the importance of DosRS$_{Mab}$ for adaptation of *Mab* to hypoxia,

highlighting a distinct regulon (compared to *Mtb)* that is significantly larger than previously described, including both genes conserved across mycobacteria as well as *Mab*-specific genes.

KEYWORDS

nontuberculous mycobacteria (NTM), *Mycobacterium abcessus*, hypoxia, two-component system (TCS), RNAseq, DosR

Introduction

Mycobacterium abscessus (*Mab*) is an opportunistic pathogen capable of causing skin, soft tissue and pulmonary infections in immunocompromised individuals and individuals with pre-existing lung disease such as cystic fibrosis (CF) and bronchiectasis (Brown-Elliott and Wallace, 2002; Olivier et al., 2003; Harris and Kenna, 2014; Lee et al., 2015; Lopeman et al., 2019). Impaired innate immune defenses and viscous mucus within the CF lung contribute to reduced clearance of bacterial pathogens leading to increased rates of infections and morbidity (Lyczak et al., 2002; Chmiel and Davis, 2003). *Mab* is the most common rapidly-growing mycobacterial (RGM) species recovered from the lungs of CF patients (Esther et al., 2010). Within the CF population and patients with underlying lung dysfunction, infections caused by *Mab* are associated with lung function decline, increased hospital visits, prolonged hospital stays and in some cases exclusion from lung transplants (Olivier et al., 2003; Esther et al., 2010; Lopeman et al., 2019). Due to *Mab's* inherent antibiotic resistance, treatment options are limited, resulting in extremely low cure rates of less than 50% (Greendyke and Byrd, 2008; Hurst-Hess et al., 2017; Molina-Torres et al., 2018; Story-Roller et al., 2018; Lopeman et al., 2019).

The development of effective treatment strategies for *Mab* is hindered by discrepancies between *in vitro* and *in vivo* susceptibilities associated with *Mab's* unique lifestyle (Greendyke and Byrd, 2008; Philley et al., 2016; Molina-Torres et al., 2018). Akin to *Mycobacterium tuberculosis* (*Mtb*), the causative agent of tuberculosis, *Mab* resides within pulmonary macrophages and within granulomas which limit antibiotic accessibility and promote drug tolerance, making treatment of an inherently antibiotic resistant pathogen even more difficult (Bernut et al., 2016; Peddireddy et al., 2017). The viscous mucus in the CF lung represents an additional hostile niche within the host to which *Mab* must adapt (Lyczak et al., 2002; Chmiel and Davis, 2003; Miranda-CasoLuengo et al., 2016; Dubois et al., 2019). One key host-derived stress encountered by *Mab* in all three of these microenvironments is decreased oxygen tension, with oxygen tension estimated to be ~1% O_2 within these niches (Worlitzsch et al., 2002; Cunningham-Bussel et al., 2013; Hudock et al., 2017). Thus, to successfully cause an infection, *Mab* must encode mechanisms to adapt and persist under hypoxic conditions. Transcriptional responses to host-derived cues/stresses are not well-defined in this NTM pathogen, requiring further studies to understand how *Mab* adapts its physiology and virulence factor expression to cause insidious, persistent infections.

Two-component signaling (TCS) is a mechanism commonly utilized by prokaryotes to regulate virulence gene expression in response to host-derived cues (Yarwood et al., 2001; Walters et al., 2006; Gonzalo-Asensio et al., 2008; Gooderham and Hancock, 2009). A typical TCS consists of a sensor histidine kinase (HK) responsible for signal recognition and subsequent phosphorylation of a cognate response regulator (RR) which binds DNA motifs within promoter regions to drive alterations in gene expression (Stock et al., 1989; West and Stock, 2001; Mascher et al., 2006; Salazar and Laub, 2015). *Mab* encodes 11 TCS, 5 orphan RRs and 1 orphan HK each with a corresponding ortholog in *Mtb*; however, in-depth studies of *Mab* TCS have not been performed (Bretl et al., 2011). The well-documented atypical TCS DosRS/T_{Mtb}, is known to control a ~50 gene regulon to counteract hypoxic and nitrosative stress encountered within macrophages and granulomas (Sherman et al., 2001; Park et al., 2003; Voskuil et al., 2003; Leistikow et al., 2010; Rohde et al., 2012; Cunningham-Bussel et al., 2013; Peterson et al., 2020; Kundu and Basu, 2021). DosRS/$T_{Mtb,}$contains 2 HKs (DosS and DosT) rather than one which are responsible for phosphorylating the RR DosR at different stages of hypoxia (Roberts et al., 2004). Although *Mtb dosT* contributes to signaling in early stages of hypoxia, it is constitutively expressed and is not part of the $DosR_{Mtb}$ regulon (Honaker et al., 2009). The $DosR_{Mtb}$ regulon includes autoregulation of *dosRS* itself, as well as heat shock proteins, triacylglycerol synthases, ferrodoxins, universal stress proteins, diacylglycerol acyltransferases, and nitroreductase which are implicated in dormancy, resuscitation, phenotypic drug tolerance and increased lipid metabolism (Park et al., 2003; Voskuil et al., 2003; Leistikow et al., 2010; Galagan et al., 2013; Aguilar-Ayala et al., 2017). Induction of *Mtb dosR* within animal models capable of forming hypoxic granulomas (rhesus macaques, guinea pigs, and C3HeB/FeJ mice) and attenuation of mutants lacking $DosRS_{Mtb}$ highlight the importance of this TCS for *Mtb* pathogenesis (Converse et al., 2009; Gautam et al., 2015a, Gautam et al., 2015b; Mehra et al., 2015).

According to whole genome sequence data, *Mab* encodes a DosR ortholog (*Mab*_3891c) with a high level of homology with $DosR_{Mtb}$ (~72% identity) adjacent to and upstream of $DosS_{Mab}$ (*Mab*_3890c) with lower similarity (~51% identify) to its counterpart in *Mtb*. *Mab* does not appear to encode a secondary orphan HK analogous to DosT, with the closest homolog to *dosT* being $dosS_{Mab}$/*Mab*_3890C (53% identity). At the time this study

was initiated, only two reports made mention of DosRS$_{Mab}$. A bioinformatics study by Gerasimova et al. used *Mtb* DosR promoter motifs to predict a small DosR$_{Mab}$ regulon consisting of only 6 genes (Gerasimova et al., 2011). A subsequent transcriptomics study by Miranda Caso-Luengo et al. demonstrated induction of the 6 predicted DosR$_{Mab}$ regulated genes plus 56 other genes upon exposure to nitric oxide (NO) (Miranda-CasoLuengo et al., 2016). It remained unclear whether induction of these genes occurs through signaling of DosRS$_{Mab}$ or whether hypoxia is an induction cue.

Although there is considerable overlap in the repertoires of TCS encoded by different mycobacteria, few cross-species transcriptomic studies are available comparing TCS regulons and regulatory networks between e.g. *Mtb* and NTM pathogens. Given the diversity of conditions encountered by *Mab* as an environmental, opportunistic pathogen, and larger genome (compared to *Mtb)* comprised of ~800 species-specific genes, the potential for unique gene sets in *Mab* TCS regulons is high (Malhotra et al., 2017; Wee et al., 2017). A hypoxia model mimicking the physiologic conditions in the mucus of CF airways, within granulomas and intramacrophage compartments was used to evaluate the role of DosRS$_{Mab}$ and assess transcriptional regulation mediated by this TCS. Our work demonstrates DosRS$_{Mab}$ is important for maximal growth and survival in hypoxia and regulates a potentially larger set of genes than previously predicted. RNAseq revealed upregulation of >1000 genes in hypoxia including 127 putative DosRS$_{Mab}$ regulated genes. Information gained from this study identifies the importance of the DosRS$_{Mab}$ TCS in adaptation to hypoxia for survival and provides valuable knowledge of a novel set of hypoxia-induced genes in this species for future studies.

Methods

Mycobacterium abscessus cloning

Mab$_{\Delta dosRS}$ was generated *via* recombineering as described by van Kessell and Hatfull in the strain *Mab* 390S obtained from the Thomas Byrd lab (Byrd and Lyons, 1999; van Kessel and Hatfull, 2007). In brief, an allelic exchange substrate (AES) was engineered containing an apramycin resistance cassette flanked by ~1000 nucleotides upstream and downstream of the *dosRS* operon *via* round the horn PCR and fast cloning (Moore and Prevelige, 2002; Li et al., 2011). *Mab*::pJV53 competent cells induced with .02% acetamide for 4 hours were electroporated with 100ng AES, recovered in 7H9 OADC media for 24 hours, and plated on 7H10 agar supplemented with apramycin 50 µg/ml. Complement strain, *Mab*$_{\Delta dosRS+C}$, containing *dosRS* with its native promoter was engineered using round the horn (Moore and Prevelige, 2002) and fast cloning (Li et al., 2011) in the integrating vector pUAB400 followed by electroporation into *Mab*$_{\Delta dosRS}$ (Singh et al., 2006). *Mab* 390S and *Mab*$_{\Delta dosRS}$ were transformed with pMV306hspG13lux (Addgene #26161) to generate the constitutive lux strains, *Mab* 390S P$_{hsp60}$-lux and *Mab*$_{\Delta dosRS}$ P$_{hsp60}$-lux. Lux reporters under the control of P$_{dosR}$ and P$_{2489}$ were constructed in the background plasmid pMV306hspG13lux to generate Mab 390S P$_{dosR}$-lux, *Mab*$_{\Delta dosRS}$ P$_{dosR}$-lux, *Mab* 390S P$_{2489}$-lux, and *Mab*$_{\Delta dosRS}$ P$_{2489}$-lux, *via* replacement of P$_{hsp60}$ (hsp60 promoter) using round-the horn cloning (Moore and Prevelige, 2002; Andreu et al., 2010; Li et al., 2011). Refer to Table S1 for strains, plasmids and primers used for cloning.

Hypoxic and re-aeration culture models

Cultures were grown in 7H9-OADC+.05% tyloxapol from glycerol stocks at 37°C while shaking unless otherwise noted. For growth kinetics assays, strains were inoculated from mid-log phase starter cultures into 13ml of media in filter-capped T-25 flasks to an OD$_{600}$ = 0.02. Hypoxic cultures were grown standing in a hypoxic incubator set at 1% O_2 while aerated controls were cultured at 20% O_2 while shaking at 100 rpm. Re-aeration studies were conducted after cultures were subjected to hypoxia or grown at 20% O_2 for 30 days. Optical density readings (OD$_{600nm}$) were taken on days 2, 3, 5, 8 and 10.

RNA experiments

RNA was extracted as previously described (Rohde et al., 2007) in triplicate from hypoxic cultures (1% O_2) and normoxic cultures (20% O_2) for qRT-PCR and RNAseq. At designated time points, cultures were pelleted at 4300 rpm for 5 minutes, resuspended in guanidine thiocyanate buffer, pelleted again at 12,000 rpm for 5 min, and stored at -80°C until processing. Thawed pellets were resuspended in 65°C Trizol then lysed using 0.1mM silicon beads in a BeadBeater at max speed for 1 minute 2x followed by cooling on ice for 1 minute between bead beating. Isolation of total RNA from Trizol lysates was performed using chloroform extraction and Qiagen RNeasy column purification. Total RNA was treated with Turbo DNase (Invitrogen) to eliminate DNA contamination. 50 ng/µl of total RNA was used to generate cDNA using iScript™ cDNA synthesis kit (Bio-Rad) for qRT-PCR reactions carried out in a QuantStudio7 thermocycler. Primers used for qRT-PCR are listed in Table S1. RNA samples for RNAseq analysis were pooled at equal RNA concentrations from three biological experiments as previously described (Tomlinson et al., 2021; Tomlinson et al., 2022) prior to library preparation at a concentration of 50 ng/µl in 20 µl. Only RNA samples with RIN>6 as determined by Tapestation analysis were utilized. RNA samples were sequenced by Microbial Genome Sequencing Center (MiGs) using Illumina sequencing protocol aligning reads to the *Mab* ATCC19977 genome (accession #CU458896). RNAseq data reflects a minimum of 12M paired end reads per sample. Due to incompatibility of Ribo-zero rRNA removal kit (Illumina) with *Mab* which resulted in high levels of rRNA, MiGS designed custom depletion probes (Table S2) for rRNA depletion. Raw data was received from MiGs as fastq files followed by analysis using CLC Genomics Workbench 12 (Qiagen Bioinformatics). Illumina paired importer tool was used to eliminate failed reads using the quality score parameter option set to Illumina Pipelines 1.8. Expression browser tool (v1.1) was used to calculate gene expression with an output of transcript per million (TPM). Differential gene expression is expressed as a $\log_2$FC of ≤-1 or ≥1 and visualized as scatter plots created in GraphPad Prism 9.

Lux reporter assays

Bio-luminescent reporter strains were grown to mid-log phase, diluted to .02 OD in 13ml in T25 flasks and grown in either 20% O_2 or 1% O_2 for 1, 5 and 20 days. 200 ul of each culture was aliquoted in triplicate into 96 well white bottomed plate to measure luminescence *via* Synergy H4 reader (Biotek). Fold change of luminescence was analyzed comparing individual strains in 1% O_2 to 20% O_2 using *Mab* 390S P_{hsp60}-lux or $Mab_{\Delta dosRS}$ P_{hsp60}-lux as internal controls (1%O_2(P_{dosR} or P_{2489}/P_{hsp60}))/(20% O_2(P_{dosR} or P_{2489}/P_{hsp60})).

Results

Growth and transcriptome remodeling of *Mab* in a defined hypoxia model

Our first goal was to develop a tractable *in vitro* model to investigate the mechanisms employed by *Mab* to persist under physiologically relevant oxygen-limited conditions. To do this, *Mab* 390S was grown under standing conditions in a 1% O_2 atmosphere to mimic the pO_2 observed within the CF lung, macrophages and granulomas (Worlitzsch et al., 2002; Cunningham-Bussel et al., 2013; Hudock et al., 2017). *Mab* 390S grew steadily at 1% O_2, reaching OD_{600} ~0.7 by day 5 with continued increase to ~0.9 by day 10 (Figure S1). Somewhat unexpectedly, the intended aerobic control culture (20% O_2 atmosphere, standing) had a very similar growth profile, reaching only a slightly higher OD ~1.2 by day 10 (Figure S1). In contrast, *Mab* 390S grown in 20% O_2 with shaking (100rpm) reached a maximum density by day 5 (OD_{600}~1.6) and subsequently plateaued up to day 10 (Figure S1). This difference is likely due to the microaerobic conditions experienced by bacilli growing below the media surface, as previously seen with *Mtb* and BCG strains grown in standing conditions (Cunningham and Spreadbury, 1998; Purkayastha et al., 2002). To maximize the contrast between aerobic and hypoxic conditions, *Mab* cultures shaking in 20% O_2 served as references for all hypoxia experiments. Thus, *Mab* is not only able to survive but to actively replicate under *in-vivo* like hypoxia conditions. It is worth noting that exposure of *Mab* to sudden hypoxia using BD Gaspack anaerobic pouches led to rapid sterilization of the cultures (data not shown). This may indicate a lower threshold of O_2 levels needed for *Mab* viability was exceeded or that slower, adaptive responses are necessary to survive.

Exploiting this model to profile *Mab* differential gene expression (DGE) in response to hypoxia, RNAseq transcriptomic analysis was conducted on wild-type *Mab* 390S cultured at 1% O_2 and 20% O_2 on day 5. This time point reflects the maximal difference in OD_{600nm} between hypoxic and aerated cultures and precedes the plateau in growth curves (Figure S1). The scatter plot in Figure 1A graphically depicts the dramatic genome-wide alterations in *Mab* 390S gene expression induced by *in vivo*-like low oxygen condition. The *Mab* hypoxia response included induction of 1,190 genes (≥ 1 log_2 fold change compared to 20% O_2) and downregulation of 1,062 genes (≤ 1 log_2 fold change compared to 20% O_2). This represented a larger set of hypoxia-induced genes than observed in *Mtb* in two studies under similar 1% O_2 hypoxia conditions (induction of ~400 genes detected *via* microarray and ~682 *via* RNAseq) (Rustad et al., 2009; Vilcheze et al., 2022). These data highlight the functional genomic differences between *Mab* and *Mtb*, in particular their distinct patterns of gene regulation in response to hypoxia which are discussed in detail below.

To identify putative regulators of hypoxia adaptation in *Mab*, we assessed the differential expression of TCSs and other annotated transcription factors in the 1% hypoxia model. Of the 11 TCS orthologous to *Mtb*, only *dosRS*, *mtrA*, *narS* and the orphan RRs *Mab_2133* and *Mab_3520c* displayed DGE (Figure 1B). *Mab_dosRS* exhibited the largest magnitude of gene induction with log_2FC of 3.9 and 4.5, respectively, pointing to $DosRS_{Mab}$ as an important TCS facilitating adaptation to hypoxic stress. The other TCS components were minimally induced with a log_2FC of 1.6 for *narS*, 1.2 for *mtrA* and 1.1 for the orphan RR *Mab_2133*. The roles of *narS, mtrA* and *Mab_2133* have not been determined in *Mab*. However, in the context of *Mtb*, the regulons of DosRS and NarLS TCS display partial overlap and protein-protein interactions between the RR from these two TCSs, DosR and NarL, have been detected (Malhotra et al., 2015). *mtrA* is essential in *Mtb* due its role in replication, whereas in *Mab mtrA* was reported to be non-essential, pointing to potential differences in the role of this TCS between the two species (Fol et al., 2006; Akusobi et al., 2022). The *Mtb* ortholog (Rv3143) of orphan RR *Mab_2133* is implicated in nitrate metabolism in the absence of oxygen, binds to *nuo* subunits required for electron transport and is within nuo operon (Plocinska et al., 2022). *Mab's* nuo operon displays synteny with the *Mtb nuo* operon including the orphan RR *Mab_2133*. Whereas Rv3143 was moderately induced by hypoxia in a DosR-dependent manner (Kendall et al., 2004), the upregulation of *Mab_2133* in our hypoxia model was not altered in the absence of DosRS (Table S3). The only TCS gene displaying substantial downregulation was *Mab_3520c* (log_2FC = -9.7). The *Mtb* ortholog of *Mab_3520c*, Rv0260c, is known to be upregulated in hypoxia and to interact with DosS *via* protein-protein interaction independent of DosR; however, the function of *Rv0260c* has not been identified (Gautam et al., 2019; Vilcheze et al., 2022). The opposite pattern of regulation of Rv0260c (induced) and *Mab*_3520c (repressed) in hypoxia implies they are utilized differently for adaptation to hypoxia. Thus, our transcriptomic analyses of *Mab* under physiologic hypoxia conditions point to *Mab* DosRS as an important TCS aiding in adaptation to hypoxia.

In addition to induction of the *Mab_dosRS* TCS, we also observed upregulation of 80 single component transcription factors (TF) in hypoxia (Table S3). Due to the high number of TF, only the genes with a log_2FC ≥ 3 are included in Table S4 with the most highly induced genes being *Mab_4180* (lclR), *Mab_2606c* (TetR family), *Mab_4332* (TetR family) and *Mab_3018* (GntR family). The *Mtb* orthologs for *Mab_4332* (Rv0273c) and *Mab_3018* (Rv0586) have 64.14% and 45.53% identity, respectively. Rv0273c has been identified as a regulator of *inhA*, an enoyl-ACP reductase involved in mycolic acid synthesis, and

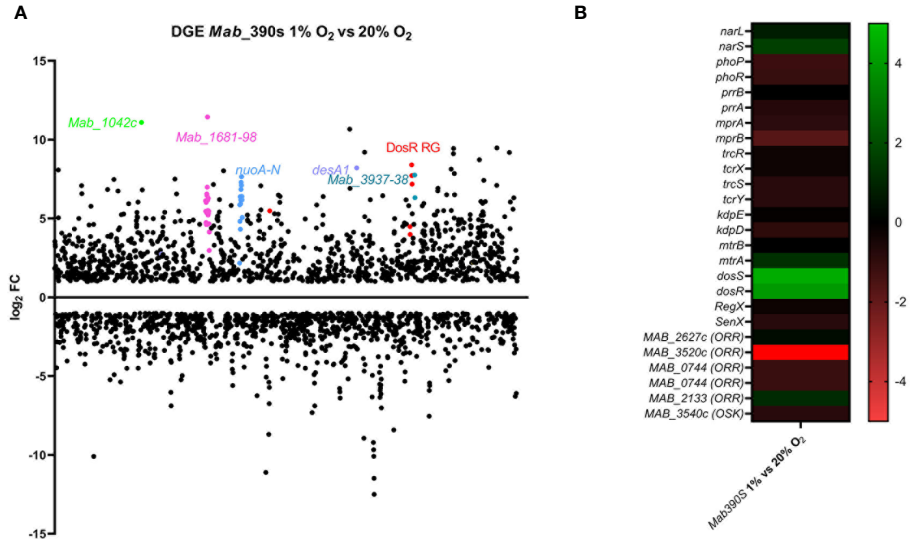

FIGURE 1
Transcriptome analysis of *Mab*390S in defined hypoxia model. DGE is visualized as **(A)** scatter plot depicting changes in gene expression reported as TPM with ≥ or ≤ log_2FC on Day 5 for *Mab* 390S 1% O_2 vs *Mab* 390S 20% O_2. Dots represent individual genes (neon green=*Mab_1042C*, pink=*Mab_1681-1698*, blue=*nuo* operon, purple= *desA1*, turquoise=*Mab_3937 & 3938*, red= predicted DosR regulated genes (RG). **(B)** Heat map showing DGE of TCS of *Mab* 390S in 1% O_2 vs 20% O_2. In gene names, orphan response regulators and orphan sensor kinases are denoted as ORR and OSK, respectively.

Rv0586 is known to mediate lipid metabolism in *Mtb* (Santangelo Mde et al., 2009; Yousuf et al., 2018; Zhu et al., 2018). Both *Mab_4180* and *Mab_2606c* share less than 30% sequence homology with the *Mtb* orthologs and no known function has been identified. Although few *Mab* transcriptional regulators have been characterized, the large number of regulators with altered expression under hypoxic stress are likely key nodes in the regulatory networks needed to adapt *in vivo*.

Due to the number of TFs and their magnitude of modulation in response to hypoxia, including upregulation of *Mab_dosRS*, the broad scope of transcriptional changes was not surprising. The list of hypoxia-induced genes included loci involved in fatty acid and cholesterol metabolism, components of the NADH-quinone oxidoreductase subunits (*nuoA-N*), 6 epoxide hydrolases (*ephD*), ATP synthase subunits, 5 mammalian cell entry operons (MCE), members of the glycopeptidolipid locus (GPL), and 520 hypothetical genes (Tables S3, 4). Several pathways critical for pathogenesis of *Mtb*, such as fatty acid and cholesterol metabolism, are also induced in various hypoxia models (Wayne model, 1% O_2) and within granulomas (Wilburn et al., 2018; Yang et al., 2021; Vilcheze et al., 2022). All four MCE loci in *Mtb* are differentially expressed in response to hypoxia, suggesting an important role for this family of lipid/cholesterol transporters in adaptation to this stress. While *mce2* and *mce3* were induced in a hypoxia model similar to ours (1% O_2, 5 days), *mce1* was repressed, and *mce4* expression remained unchanged (Vilcheze et al., 2022). A separate study by Rathor et al. found that *mce4* was upregulated after much longer durations of hypoxia stress (Rathor et al., 2016). Mce1 and Mce4 are known to play a role in the transport of fatty acids and cholesterol (Wilburn et al., 2018; Klepp et al., 2022), whereas the function of Mce2 and Mce3 have not been determined yet. In contrast, five of the seven MCE systems encoded by *Mab* were upregulated in 1% O_2 after 5 days (Tables S3, 4). Although the biological role of MCE complexes in *Mab* have not been studied, their distinct expression profile suggest they may be important for *in vivo* survival. The *Mab* hypoxia-induced gene set also included a large number of genes implicated in β-oxidation pathways - 14 *fadE* genes, 8 *fadD* genes, and one of each *fadA* and *fadH* (Tables S3, 4). Upregulation of 6 *ephD* genes (an epoxide hydrolase predicted to alter the amount of epoxymycolates in the cell wall), members of the GPL locus accounting for smooth morphology (Tables S3, 4), and arabinosyltransferases A and B (Supplemental Table 1) involved with arabinogalactan synthesis indicate *Mab* may undergo cell wall remodeling in response to hypoxia (Amin et al., 2008; Gutierrez et al., 2018; Madacki et al., 2018).

In addition to β-oxidation, metabolic pathway induction included *nuo* subunits *A-N*, ATPase subunits, and cytochrome P450 genes (Tables S3, 4). NuoA-N are subunits of the proton pumping NADH dehydrogenase type 1 responsible for transferring electrons to menaquinone in the electron transport chain (ETC) in an energy conserving manner to generate a PMF (Weinstein et al., 2005). Although these genes are upregulated in the RGM *Mycobacterium smegmatis* (*Msmeg)* during slowed growth and in *E.coli* in anaerobic conditions, this is not a feature observed in the hypoxic response of slow-growing mycobacteria (SGM) like *Mtb* (Unden and Bongaerts, 1997; Berney and Cook, 2010). In contrast to *Mab*, the nuo operon and ATPase subunits are downregulated in hypoxic *Mtb*, further highlighting the distinct stress responses and energy metabolism of these two species in response to hypoxia (Cook et al., 2014; Vilcheze et al., 2022). Of the 25 *Mab* cytochrome P450s, 14 were induced in hypoxia (Supplemental Table 1). This data is consistent with hypoxic induction a large number of

cytochrome P450s in the RGM *Msmeg* but not in the SGM *Mtb* with the exception of only 2 cytochrome P450s (Sherman et al., 2001; Berney and Cook, 2010; Ortega Ugalde et al., 2019). The roles of individual *Mab* cytochrome P450s remain unknown but the functions of the *Mtb* orthologs are dependent on their ferredoxin redox partners and include cholesterol degradation, redox balance, and virulence (Capyk et al., 2009). Our data supports hypoxic induction of 2 ferredoxins (*Mab_0914c* & *Mab_2049c*) and 3 ferredoxin reductases (*Mab_0930*, *Mab_2047c* and *Mab_4356c*) (Table S3). Induction of *nuo*A-N, ATPAse subunits, the large number of cytochrome P450s and ferredoxins implies *Mab* may employ different sets of genes for anaerobic respiration in its response to hypoxia and adapation.

Mab's transcriptional adaptation to hypoxia also comprised a large set of downregulated genes including but not limited to multiple TF, tRNAs, 30S and 50S ribosomal proteins, alternative sigma factors, and 431 hypothetical proteins (Table S3). Downregulation of genes involved in essential processes such as protein synthesis (e.g. tRNAs, ribosomal proteins and sigma factors) are consistent with the slowed growth observed in hypoxic *Mab* cultures. Included among the most downregulated genes in hypoxia (Table S3) is the orphan response regulator *Mab_3520c* (Figure 1B) and three adjacent upstream genes (nirD/MAB_3521c, nirB/MAB_3522c), and nark3/MAB_3523c) predicted to be involved in nitrite reduction and extrusion (Malm et al., 2009). *Mtb nirB* and *nirD* orthologs are reportedly induced in nutrient starvation but minimal to no DGE occurred in hypoxia at 1% O_2 (Vilcheze et al., 2022). However, in the Wayne model of hypoxia *Mtb nirB* displayed induction and functional *nirBD* genes were required for growth in hypoxia when nitrite was used as the sole nitrogen source (Akhtar et al., 2013).

Construction and validation of $Mab_{\Delta dosRS}$ and $Mab_{\Delta dosRS+C}$

Elucidation of the global transcriptional responses of *Mab* to hypoxia for the first time revealed the DosRS TCS is employed during hypoxic adaptation, yet much remains unknown about the role of DosRS in gene regulation and *Mab* pathogenesis. The $DosR_{Mab}$ regulon was previously predicted to consist of only 6 genes - *Mab_3890* (*dosS*), *Mab_3891* (*dosR*), *Mab_2489* (universal stress protein, USP), *Mab_3902c* (ortholog of Rv2004c), *Mab_3903* (nitroreductase) and *Mab_3904* (USP) – based solely on bioinformatic analysis (Gerasimova et al., 2011). However, at the time this study was initiated, the role of $DosRS_{Mab}$ signaling in gene regulation, including induction of this gene set, remained to be experimentally demonstrated. To enable determination of the $DosRS_{Mab}$ regulon and role of this TCS in *Mab* adaptation to hypoxia, we generated $Mab_{\Delta dosRS}$(knockout mutant) using recombineering and the corresponding complemented strain ($Mab_{\Delta dosRS+C}$) expressing a single, integrated *dosRS* allele driven by its native promoter (van Kessel and Hatfull, 2007). In addition to confirming strain genotypes by PCR and DNA sequencing (data not shown), the absence of *dosRS* transcripts in $Mab_{\Delta dosRS}$ and restoration to wild-type levels in $Mab_{\Delta dosRS+C}$ was validated by qRT-PCR (Figure 2A). We next assessed transcript levels of 4 genes (in addition to *dosRS* operon itself) previously predicted to be DosR-dependent. Loss of a functional DosRS system resulted in down-regulation of all predicted $DosR_{Mab}$-regulated genes by >2 log (*MAB_2489, MAB_3902c, MAB_3903)* or > 1 log in the case of *MAB_3904* with restoration to wild-type levels in the complemented strain (Figure 2B), consistent with DosR-mediated induction of these genes.

$DosRS_{Mab}$ is required for maximal growth in hypoxia

As detailed above, to verify the role of DosRS under *in vivo* relevant conditions, we compared the growth kinetics assays of *Mab* 390S, $Mab_{\Delta dosRS}$, and $Mab_{\Delta dosRS+C}$ in hypoxic (1% O_2, standing) versus aerobic (20% O_2, shaking) conditions. Strains were monitored over a 30-day period using CFU/ml as the readout at day 5, 20, and 30 and grown in normoxic conditions after plating. Cultures grown in 20% O_2 reached maximum growth on day 5 with no difference in

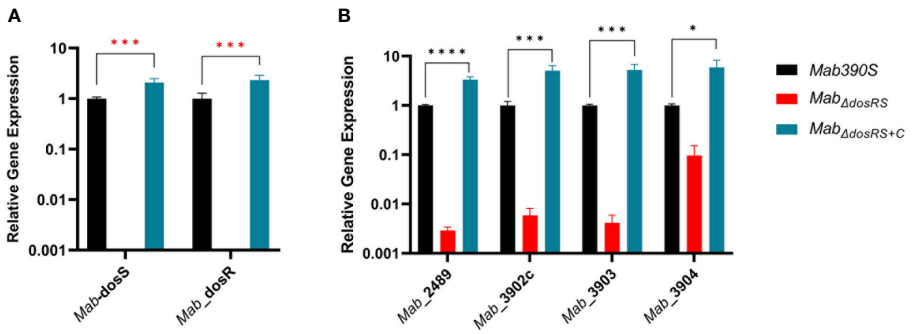

FIGURE 2
Validation of $Mab_{\Delta dosRS}$ and $Mab_{\Delta dosRS+C}$. qRT-PCR was performed to **(A)** confirm the deletion and restoration of *dosS* and *dosR* in $Mab_{\Delta dosRS}$ and $Mab_{\Delta dosRS+C}$, respectively, and **(B)** assess the effect on predicted downstream genes. *Mab 390S* (black), $Mab_{\Delta dosRS}$ (red) and $Mab_{\Delta dosRS+C}$ (blue). Data is representative of 3 experiments performed in triplicate. *P* values were calculated *via* one -way ANOVA using GraphPad. Red stars indicate C_t values were not detected for *Mab dosR* nor *dosS* in the mutant strain. **P*-value <.05, ****P*-value <.001 *****P*-value <.0001.

growth between strains at any time point confirming fully aerated cultures are not dependent on DosRS for replication (Figure 3A). At 1% O_2 maximum growth was achieved by day 20 in *Mab* 390S with a ~2-log decrease in $Mab_{\Delta dosRS}$and ~log decrease in $Mab_{\Delta dosRS+C}$ (Figure 3B) suggesting a functional DosRS is required for maximal growth and survival during hypoxic stress. By day 30 in 1% O_2, *Mab* 390S displayed a slight decrease in CFU compared to day 20 however, this decline was also observed in fully aerated cultures indicating that hypoxic stress was not the cause (Figures 3A, B). These data support the conclusion that $DosRS_{Mab}$ is necessary for growth in hypoxic environments that mimic the physiologic environments of the CF lung, within macrophages and granulomas (Worlitzsch et al., 2002; Cunningham-Bussel et al., 2013; Hudock et al., 2017). Unexpectedly, a morphotype transition from smooth to rough occurred in $Mab_{\Delta dosRS}$ after pro-longed exposure to 1% O_2. On day 20 and 30 an observable change in morphology occurred only in the mutant strain resulting in a heterogenous population of smooth and rough colonies (Figures 4A–D), indicating a DosR-dependent inducible alteration in cell wall composition for $Mab_{\Delta dosRS}$. This is corroborated by the fact that in hypoxic liquid culture assays, $Mab_{\Delta dosRS}$ alone adopted a biofilm-like pellicle layer that was resistant to disruption, whereas other strains maintained a homogeneous composition (data not shown).

Prompted by the inability of $Mtb_{\Delta dosR}$ to resuscitate after re-aeration from hypoxia (Leistikow et al., 2010; Veatch and Kaushal, 2018), we investigated the ability of $Mab_{\Delta dosRS}$ to resuscitate after 30 days in hypoxia. Day 30 cultures taken from 20% O_2 and 1% O_2 were diluted to an OD_{600nm} of 0.02 and grown in 20% O_2 while shaking to evaluate the recovery of $Mab_{\Delta dosRS}$ after prolonged exposure to hypoxia. OD_{600nm} was taken over a 10-day period (Day 0, 2, 3, 5, 8, and 10) to monitor growth kinetics after re-introduction of O_2. All strains originating from aerobic conditions displayed similar growth curves after re-culturing and reached maximal OD by day 5 (Figure 5A). In contrast, after being subjected to hypoxia for 30 days, $Mab_{\Delta dosRS}$ displayed reduced growth compared to *Mab* 390S and $Mab_{\Delta dosRS+C}$ taken from 1% O_2 (Figure 5B). Attenuated growth in 1% O_2 and the inability to resuscitate after re-aeration for $Mab_{\Delta dosRS}$ supports a critical role for $DosRS_{Mab}$ in mediating adaptation to changing oxygen levels encountered within the host during both dormancy and reactivation.

Identification of a large and unique gene set regulated by $DosRS_{Mab}$

We next analyzed DGE between *Mab*390S and $Mab_{\Delta dosRS}$ in hypoxia *via* RNAseq to experimentally identify DosRS regulated genes (Figure 6A). Cultures of *Mab* 390S and $Mab_{\Delta dosRS}$ were grown at 1% O_2 for 5 days at which point RNA was extracted from three independent experiments for analysis. In the absence of DosRS, 216 genes were expressed at lower levels relative to *Mab* 390S after exposure to 1% O_2 (Figure 6A), of which 127 genes were also induced in *Mab* 390S by hypoxia (Table S3). This pattern is consistent with DosRS-dependent hypoxia induction, suggesting that *Mab* DosR may control a much larger regulon than previously predicted. In subsequent analyses, we defined putative DosRS-dependent hypoxia induced genes as those whose transcript levels were decreased by $\log_2FC \geq 1$ in the $Mab_{\Delta dosRS}$ in 1% O_2 and were induced by $\log_2FC \geq 1$ in *Mab* 390S 1% O_2 (Table S3). The top 20 putative DosRS-dependent genes induced most highly by hypoxia (Table S5) include 4 of the genes previously predicted *in silico* to be members of the $DosRS_{Mab}$ regulon. Notably, two of the most highly upregulated genes, *Mab_3937* and *Mab_3354* (*desA1*), appear to be *Mab*-specific members of this regulon. *Mab_3937*, a hypothetical protein with no known ortholog, is predicted to be in an operon with *Mab_3938* and *Mab_3939*, encoding a clp protease subunit (ClpC2) with orthologous counterparts in *Mtb* and *Msmeg* which are essential genes. (Sassetti et al., 2003; Miranda-CasoLuengo et al., 2016; Kester et al., 2021). Both *desA1* (*Mab_3354*) and *desA2* (*Mab_1237*), desaturase enzymes with predicted roles in the biosynthesis of the mycolic acid component of mycobacterial cell walls, exhibited hypoxic DGE in the *dosRS* mutant (Yeruva et al., 2016; Bailo et al., 2022). Recently *desA2* but not *desA1* was predicted to be an essential gene in *Mab*, *Mtb* and *Msmeg* suggesting even slight downregulation could lead to detrimental alterations in the cell wall (Akusobi et al., 2022; Bailo et al., 2022). Although *Mtb* has orthologs of these genes (ClpC2, *desA1*, and *desA2)*, there is no evidence of regulation by $DosR_{Mtb}$, illustrating the potential for conserved TCS to interact with conserved target genes in distinct ways. Additionally, no known $DosR_{Mtb}$-regulated genes have been deemed essential, further highlighting the unique nature of $DosRS_{Mab}$-mediated hypoxia response. Among the 127 hypoxia-

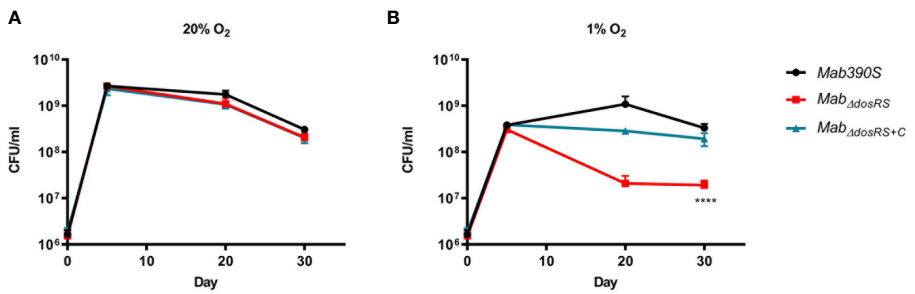

FIGURE 3
$Mab_{\Delta dosRS}$ is attenuated in hypoxia. Growth kinetics in hypoxia were assessed *via* serial dilutions, spot plating and enumeration of CFU/ml on day 5, 20 and 30. **(A)** Growth kinetics at 20% O_2 **(B)** Growth kinetics at 1% O_2. *Mab 390S* (black), $Mab_{\Delta dosRS}$ (red) and $Mab_{\Delta dosRS+C}$ (blue). Data reflects 3 independent experiments performed in triplicate. *P*-values were calculated *via* one-way ANOVA using GraphPad, ****P-value <.0001.

10.3389/fcimb.2023.1144210

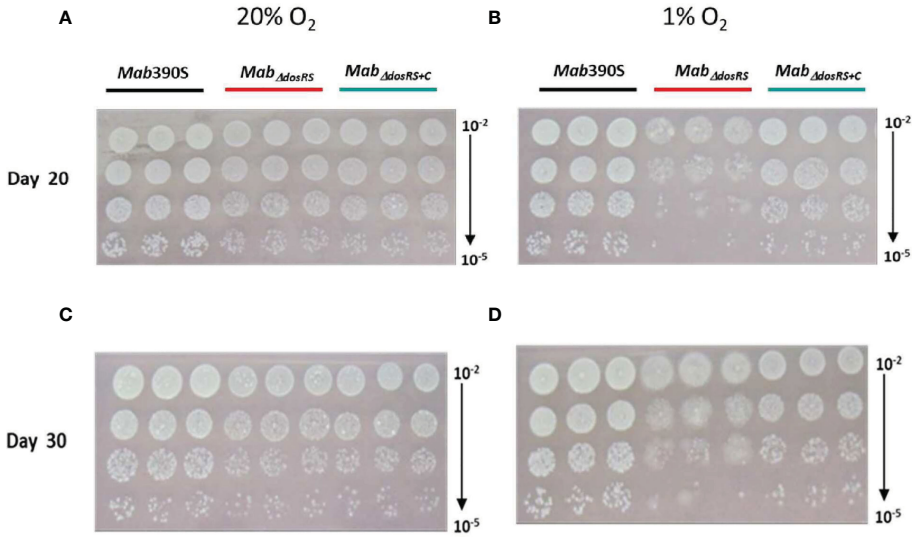

FIGURE 4
Hypoxia-induced morphological changes in $Mab_{\Delta dosRS}$. Cultures grown at 20% or 1% O_2 were spot plated on Day 20 and Day 30 and incubated under normoxic conditions. **(A)** Day 20 at 20% O_2 **(B)** Day 20 at 1% O_2 **(C)** Day 30 at 20% O_2 **(D)** Day 30 at 1% O_2.

induced putative $DosR_{Mab}$-dependent genes is a large gene cluster (*Mab_1681-1698)* containing hypothetical proteins, daunorubicin resistance efflux pump subunit (*drrA)*, and a putative *mce* operon (Table S5). Whereas some putative *Mab* MCE gene clusters have clear orthologs in *Mtb* (e.g. MAB_4146c-4155c with Mce4, Rv3492c-3501c), the predicted *Mab* MCE proteins encoded by MAB_*1681-1698* do not directly correspond to a specific MCE loci in *Mtb*. Rather, they share low homology with components of different *Mtb* MCE complexes, necessitating further research to fully assess the role of this *Mab*-specific MCE during hypoxia.

Comparing the ~ 50 genes of the $DosR_{Mtb}$ regulon with the putative $DosR_{Mab}$ regulated genes identified in this study (Supplemental Table 3), we only discovered 6 shared orthologs including 4 conserved hypothetical proteins (CHPs) plus DosR (*Mab_3891c*) and DosS (*Mab_3890c)*. In addition to the transcriptional regulator *Mab_3891c*, we found nine other transcriptional regulators to be induced by hypoxia in a putative DosR-dependent manner (Tables S3–5) with none of their *Mtb* orthologs regulated by $DosR_{Mtb}$. The transcriptional response of Mab to hypoxia is further differentiated from Mtb by the lack of regulation of any of the 7 putative triacylglycerol synthases (Tgs) by hypoxia or DosR, a characteristic of in vitro dormancy and hypoxia for Mtb (Table S3) (Voskuil et al., 2004; Deb et al., 2009). Hypoxic *Mtb* positively regulates *tgs1 via* DosR for synthesis of triacylglycerol (TAG) for energy storage and utilization. The absence of $DosR_{Mab}$ mediated induction of any Tgs enzymes under hypoxic stress points to a different mechanism for energy storage and utilization in *Mab* vs *Mtb* (Park et al., 2003; Daniel et al., 2004). The scope of the *Mab* DosR regulon precludes a comprehensive discussion of every downstream gene, many of which encode uncharacterized conserved hypothetical proteins. However, this RNAseq dataset is evidence for a species-specific regulon larger than predicted bioinformatically that likely contains novel mechanisms of hypoxia adaptation and pathogenesis.

Comparative transcriptomics also revealed upregulation of 200 genes in $Mab_{\Delta dosRS}$ compared to *Mab* 390S (Figure 6A and Table S3),

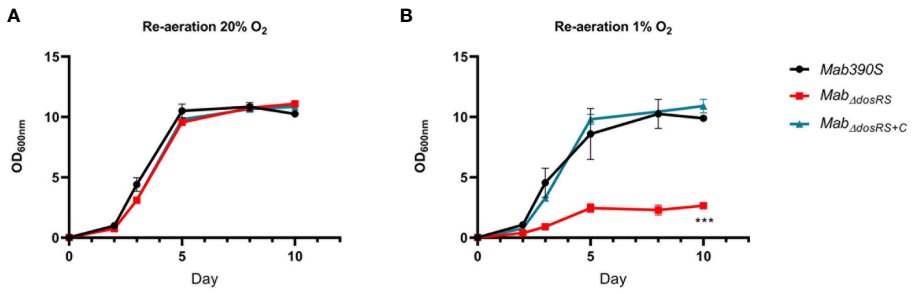

FIGURE 5
DosRS is required for resuscitation after hypoxia. OD_{600nm} was taken over a 10-day period of re-aerated cultures after 30 days of growth in either **(A)** 20% O_2 or **(B)** 1% O_2. *Mab390S* (black), $Mab_{\Delta dosRS}$ (red) and $Mab_{\Delta dosRS+C}$ (blue). Data reflects 2 independent experiments performed in triplicate. *P*-values were calculated *via* one-way ANOVA using GraphPad, ****P*-value <.001.

10.3389/fcimb.2023.1144210

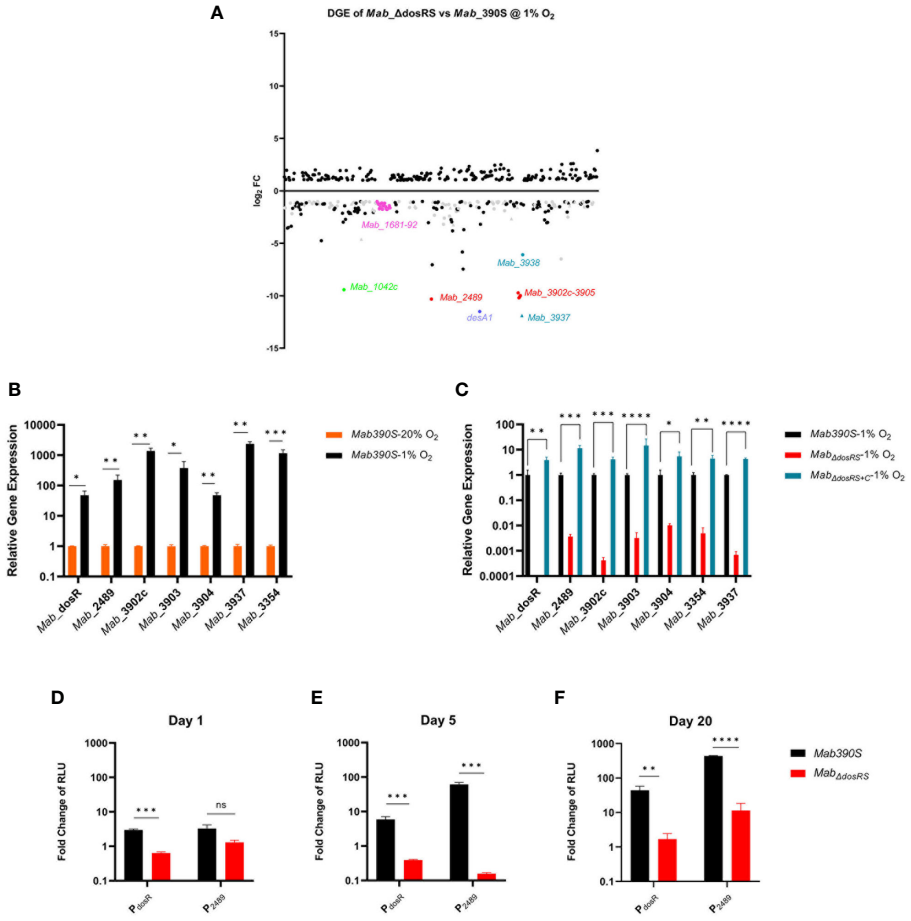

FIGURE 6
Mab DosR dependent DGE in 1% O_2. **(A)** Scatter plot of RNAseq analysis of $Mab_{\Delta dosRS}$ vs *Mab* 390S after 5 days in 1% O_2. Figure shows genes with $log_2FC \leq -1$ and ≥ 1. Gray circles are conserved hypothetical genes and gray triangles are *Mab* genes with no ortholog in *Mtb*. Names of select genes of interest are labeled (neon green=*Mab_1042C*, pink=*Mab_1681-1698*, purple= *desA1*, turquoise (triangle denotes no known ortholog in *Mtb*) =*Mab_3937 & 3938*, red= predicted DosR regulated genes (RG). **(B, C)** qRT-PCR assessment of select DosR-dependent genes. Gene expression was calculated as relative quantitation *via* the $2^{-\Delta\Delta Ct}$ method using *sigA* as the reference gene. **(B)** Hypoxia induced gene expression. Transcript levels of select genes in *Mab* 390S 20% O_2 (orange bars) and *Mab* 390S 1% O_2 (black bars). **(C)** DosR dependent gene expression. Transcript levels of select genes in $Mab_{\Delta dosRS}$ (red bars) and $Mab_{\Delta dosRS+C}$(blue bars) were compared to *Mab* 390S (black bars) in 1% O_2 on Day 5. **(D-F)** Kinetics of DosR-dependent gene induction measured luciferase reporter assays. Promoter activity in 1% O_2 was quantified by measuring luminescence compared to 20% O_2 cultures and normalized to lux-hsp60 constitutive promoter as a reference signal, $(1\%O_2(P_{dosR}$ or $P_{2489}/P_{hsp60}))/(20\%\ O_2(P_{dosR}$ or $P_{2489}/P_{hsp60}))$ and expressed as fold change of relative light units (RLU) **(D)** 24hours, **(E)** Day 5, and **(F)** Day 20. *Mab* 390S (black bars) and $Mab_{\Delta dosRS}$ (red bars). qRT-PCR and luciferase assay data are representative of 3 independent assays performed in triplicate. *P*-values were calculated using t-test **(B, D–F)** and one-way ANOVA **(C)**. *P*-values were calculated *via* GraphPad, **P*-value <.05, ** *P*-value <.01, ****P*-value <.001, *****P*-value. Not significant is denoted as ns.

however the magnitude of induction was low ranging between log_2FC of 1-3.6. Among the upregulated genes are 81 hypothetical proteins, 5 transcription factors, 30S and 50S ribosomal proteins. Included in the top 20 most highly induced genes in $Mab_{\Delta dosRS}$ are *Mab_3521c* (nitrite reductase) and *Mab_3523c* (nitrite extrusion protein) which were observed to be highly downregulated in hypoxic *Mab* 390S (Table S3). These data suggests that DosRS may act as a repressor of a subset of genes in hypoxic conditions, a hypothesis that remains to be experimentally validated. The low-level induction of other genes in the knockout strain may also result from indirect effects of DosRS on mycobacterial physiology under hypoxic stress.

To validate RNAseq results, two of the putative *Mab* DosR-dependent genes most differentially expressed in the mutant strain (*Mab_3354* and *Mab_3937*) were assessed *via* qRT-PCR along with 5 of the predicted *Mab* DosR genes (Figures 6B, C). Similar to RNAseq studies, the effect of hypoxia on gene expression was assessed in *Mab* 390S (1% vs 20% O_2) and the requirement for DosRS for DGE in response to hypoxia by comparing *Mab* 390S, $Mab_{\Delta dosRS}$ and $Mab_{\Delta dosRS+C}$. All genes assessed *via* qRT-PCR were induced by ≥ 10-fold in 1% O_2 compared to 20% O_2 for *Mab* 390S with *Mab_3937*, *Mab_3902c*, and *Mab_3354* having the highest gene induction consistent with RNAseq results (Figure 6B). These same genes displayed loss of induction in $Mab_{\Delta dosRS}$ by ≥ 10-fold similar to RNAseq results with restoration by $Mab_{\Delta dosRS+C}$ in hypoxia (Figure 6C). The most dramatic change in gene expression in $Mab_{\Delta dosRS}$ was *Mab_3902c* and *Mab_3937* with > 100-fold reduction compared to *Mab* 390S. Results from qRT-PCR corroborate RNAseq results and accentuate the magnitude of differential gene expression of predicted and newly discovered hypoxia-induced $DosRS_{Mab}$ regulated genes.

In addition to qRT-PCR, bacterial luciferase (Lux) reporter strains were used to evaluate the kinetics of hypoxia-dependent changes in gene expression across a broader time course. The integrating shuttle plasmid pMV306 luxG13 optimized for mycobacteria consists of the constitutive P_{hsp60} and P_{G13} promoters driving expression of *luxAB* and *luxCDE*, respectively (Andreu et al., 2010). Lux reporter constructs in which the constitutive P_{hsp60} promoter was replaced with promoters from two hypoxia inducible genes, DosR and *Mab*_2489 (P_{DosR} and P_{2489}) were introduced into *Mab* 390S and $Mab_{\Delta dosRS}$. Reporter assays performed on Days 1, 5, 20 identified temporal changes in gene expression with both promoters for *Mab* 390S but not in $Mab_{\Delta dosRS}$ (Figures 6D–F). The lux reporter under the control of P_{dosR} shows sustained induction over time, indicating that *dosR* is expressed throughout early and late stages of hypoxia, a trait not observed in *Mtb* (Rustad et al., 2008). Although the *Mab* 390S P_{2489}-lux reporter displays modest induction of ~ 3-fold change on day 1, there is not a significant difference compared to $Mab_{\Delta dosRS}P_{2489}$ (Figure 6D). However, on days 5 and 20 *Mab* 390S P_{2489}-lux was highly induced compared to $Mab_{\Delta dosRS}$ P_{2489}-lux with fold changes of 61 and 433, respectively (Figures 6E, F). It should be noted that $Mab_{\Delta dosRS}$ P_{2489}-lux did exhibit low-level induction on Day 20, which may be attributable to the activity of other transcription factors. However, as noted previously, there was a significant difference compared to the expression of P_{2489} in wild-type *Mab* 390S. Lux reporters facilitated dynamic monitoring of DosRS activation by hypoxia and provide a valuable tool to explore DosR-mediated gene regulation *in vitro* and *in vivo* in response to various stresses (e.g. NO, CO, antibiotics) or host microenvironments (e.g intramacrophage, granuloma, airway mucus).

Discussion

Infections caused by *Mab*, particularly within the CF population, are a major cause of concern due to the lack of efficacious antibiotics and the resulting inability to clear the infections from the airways. The poor correlation between *in vitro* drug susceptibility profiles and *in vivo* efficacy when treating *Mab* infections suggest that host-driven adaptations of *Mab* may contribute to treatment failures (Nessar et al., 2012). Host-derived cues encountered by *Mab* within the viscous mucus layer of CF airways, phagosomal compartments of macrophages, and during residence within granulomas may trigger upregulation of antimicrobial resistance mechanisms (Lyczak et al., 2002; Worlitzsch et al., 2002; Cunningham-Bussel et al., 2013; Hudock et al., 2017). Extrapolating from studies on *Mtb* (Gold and Nathan, 2017; Boldrin et al., 2020; Joshi et al., 2021), *in vivo* stresses such as hypoxia may also promote the development of phenotypically drug-tolerant persisters. Thus, a better understanding of *Mab's* physiological states and stress responses required for long-term persistence within the human host may lead to more effective treatment strategies.

Successful bacterial pathogens like *Mtb* and *Mab* employ extensive repertoires of transcription factors, including TCS, for coordinating gene expression to counteract host antimicrobial factors and immune pressure. The transcriptional regulatory networks and role of TCS of *Mtb* have been extensively characterized in multiple *in vitro* and *in vivo* models of infection (Bacon and Marsh, 2007; Rohde et al., 2012; Li et al., 2019; Stupar et al., 2022; Vilcheze et al., 2022). In contrast, few transcriptomic studies defining *Mab* stress responses, or the role of specific transcription factors have been reported (Miranda-CasoLuengo et al., 2016; Dubois et al., 2019). Given the well-documented relevance of hypoxia during *Mab*-host interactions (e.g. mucus of CF airway, macrophage phagosome, granuloma) (Lyczak et al., 2002; Worlitzsch et al., 2002; Cunningham-Bussel et al., 2013; Hudock et al., 2017), we sought to identify molecular mechanisms that enable *Mab* to adapt to these low-oxygen niches. In the better characterized pathogen *Mtb*, the master regulator of hypoxia adaptation is the atypical TCS DosRS/T, which regulates a ~50 gene regulon upon induction by hypoxia and NO stress (Park et al., 2003; Voskuil et al., 2003). *Mab* encodes orthologs of eleven of the twelve TCS found in *Mtb*, including DosRS (*dosT* homolog missing). However, as detailed in this study, the scope and content of *Mab* regulons controlled by these TCS may be less conserved. Prior to initiation of our study, only two reports had mentioned *Mab* DosRS: i) a bioinformatics study predicting a 6 gene regulon based on previously known *Mtb* DosR binding motifs (Gerasimova et al., 2011) and ii) transcriptomic study assessing the affect of NO exposure on the predicted genes (Miranda-CasoLuengo et al., 2016). These studies, however, did not directly demonstrate DosRS-mediated regulation of the predicted genes, define the transcriptional response of *Mab* to hypoxia nor the full extent of the DosR regulon, or identify a DosRS phenotype. To begin to address these knowledge gaps we developed a hypoxic model of 1% O_2 to mimic physiologically relevant oxygen tensions *Mab* encounters *in vivo* (Worlitzsch et al., 2002; Cunningham-Bussel et al., 2013; Hudock et al., 2017) to assess transcriptomics and growth kinetics of *Mab* in the presence or absence of $DosRS_{Mab}$.

Genome wide transcriptomics identified DosRS as the main TCS activated during hypoxia and analysis of a defined mutant lacking DosRS revealed a potentially larger regulon than previously predicted. We identified 216 genes to be downregulated in $Mab_{\Delta dosRS}$versus *Mab* 390S, 127 of which were upregulated in hypoxia. This gene set was deemed the putative hypoxia-induced DosR regulon-*Mab_3902c*, *Mab_3903* and Mab_*3904*), 2 novel genes displaying the highest DGE (MAB_3937 and *desA1*), 9 transcription factors, and 57 hypothetical genes among others. 22 of the 57 hypothetical genes are species-specific, further illustrating the unique nature of the regulons controlled by orthologous TCS. Not only is the *Mab* DosRS regulon likely larger than previously predicted, but it also appears to be notably larger than the well-studied *Mtb* DosR regulon. Surprisingly, the only orthologs in common between the *Mtb* DosR and *Mab* DosR regulons were the 6 genes originally predicted from the bioinformatics study and *Mab_1040*, an ortholog of the hypothetical protein *Rv3129* which is documented as an antigen in tuberculosis patients with latent infections (Park et al., 2003; Black et al., 2009; Lin et al., 2009). One of the hallmarks of *Mtb* hypoxia adaptations *in vivo* and *in vitro* is the marked upregulation of *tgs1* for energy storage and utilization (Garton et al., 2008; Deb et al., 2009). The induction of *Mab_3551c*, the primary TAG synthase gene in *Mab* (Viljoen et al.,

2016), is not observed in our *Mab in vitro* hypoxia model, suggesting *Mab* mechanisms of hypoxia adaptation or cues for regulation of lipid storage are distinctive from *Mtb*. Studies are underway to discriminate between genes whose expression is altered directly by DosR (DosR binding to promoter) versus indirectly (promoter regulated by secondary TF).

During the course of our study, Belardinelli et al. also reported on characterization of the *Mab* DosR regulon as part of efforts to repurpose antimalarial drugs that inhibit *Mtb* DosR as therapeutics for *Mab* (Belardinelli et al., 2022). Their transcriptomic comparison of *Mab* ATCC 19977 and $Mab_{\Delta dosRS}$ in microaerobic conditions identified 180 genes downregulated in a DosRS-dependent manner. Of these 180 genes, only 45 overlapped with our list of 216 genes downregulated in the *dosRS* mutant at 1% O_2. Both studies included the 6 previously predicted genes and the 2 genes most highly differentially expressed on our list (*Mab_3937*, *desA1*) plus 37 other genes. Of the 45 genes in common between these 2 studies, Belardinelli et al., reported 38 DosR binding motifs supporting the assertion that *Mab* DosR regulon is larger than previously predicted. Discrepant findings between this report and our study could be attributable to differences in strains (ATCC 19977 vs 390S), hypoxic models (20% O_2 standing vs 1% O_2 standing), time points (24hr vs 5 days), or media (Dubos-Tween albumin vs 7H9-OADC+.05% tyloxapol). Regardless, both clearly highlight the broad scope and unique nature of the $DosRS_{Mab}$ regulon and provide a framework for future studies to fully elucidate the role of this important two-component system.

The importance of DosR-regulated genes for hypoxia adaptation was evident from growth deficits seen on day 20 and 30 and impaired resuscitation after reaeration in $Mab_{\Delta dosRS}$ compared to *Mab* 390S (Figure 3). *Mab_ΔdosRS* differentially expressed genes in hypoxia contain 7 genes predicted to be essential in a recent TnSeq study under aerobic conditions (Akusobi et al., 2022), possibly accounting for these phenotypes. Included in this list is *desA2*, a desaturase enzyme that is responsible for mycolic acid biosynthesis and is essential for growth in the RGM *Msmeg* (Bailo et al., 2022). Strong induction of *desA1* in hypoxia suggests that it, along with *desA2*, may play role in cell wall modification in response to this stress. It is worth noting that, despite exclusion from the list of *Mab* predicted essential genes, the orthologous desaturase in *Msmeg* was deemed essential (Singh et al., 2016). Additionally, the MCE operon *Mab*_1693-*Mab*_1698 was differentially expressed in the mutant strain and may contribute to decreased importation of mycolic acids further disrupting cell wall integrity. The 6 other predicted essential genes possibly contributing to the $Mab_{\Delta dosRS}$ growth phenotype are 2 conserved hypothetical proteins (*Mab_3268c-Mab_3269c*), a DNA helicase (*Mab_3511c*), a protoporphyrinogen oxidase, a prephenate dehydratase (*Mab_0132*), and phosphoribosylformylglycinamidine synthase (*Mab_0698*).

In addition to growth/survival deficits and the inability to resuscitate, we also observed DosRS-dependent hypoxia-induced morphological changes. After 20 days in hypoxia, $Mab_{\Delta dosRS}$ displayed heterogeneous morphology consisting of smooth and rough colonies. This phenotype was not present in strains expressing DosRS or in fully aerated cultures, evidence that this TCS mediates dramatic remodeling of the cell wall in response hypoxia. The smooth and rough morphotypes of *Mab*, reflective of different compositions of the outer cell wall, have been shown to impact interactions with macrophages, immune stimulation and inflammation, antibiotic susceptibility, and virulence (Jonsson et al., 2007; Catherinot et al., 2009; Ruger et al., 2014; Roux et al., 2016; Li et al., 2020). Rough strains are able to trigger apoptosis of macrophages and grow extracellularly as aggregates known as cords, and are associated with worse clinical outcomes (Li et al., 2020) Mechanisms involved in smooth to rough transitions have not been fully elucidated. However, genomic comparisons between the two morphotypes revealed SNPs and indels in the *gpl* locus and in *mmpl4b* and *mps1* genes (Pawlik et al., 2013). In addition to total or partial loss of GPL due to mutations affecting its biosynthesis or transport, recent studies including identification of GPL+ rough clinical isolates suggest other mechanisms may also govern S➔R morphotype switching (Gutierrez et al., 2021). For example, Daher et al. reported that glycosylation patterns of GPL can alter *Mab* surface properties (Daher et al., 2022). An inducible transition from smooth to rough was also observed following exposure to subinhibitory doses of aminoglycoside antibiotics providing evidence for transcriptional modulation of morphotype in response to stress (Tsai et al., 2015). Belardinelli et al. reported no differences in GPL content between *Mab* ATCC 19977 and isogenic *ΔdosRS* mutant after microaerobic culture for 24 hours (Belardinelli et al., 2022). Our observation of a switch to rough morphotype in a *ΔdosRS* mutant after extended culture at 1% O_2 may reflect either adaptive cell wall remodeling triggered by lower O_2 levels or longer duration of stress in our model. Alternatively, rather than affecting GPL levels per se, inactivation of the DosRS regulon may impact GPL modifications or biosynthesis of unique cell wall constituents. Intriguingly, Pawlik et al. reported that expression of *dosR* was elevated in an R versus S strain (Pawlik et al., 2013). This seems to contrast with our data suggesting that DosRS positively regulates GPLs, or at least the smooth phenotype (e.g. loss of DosRS➔rough phenotype in hypoxia). Whether this is a direct correlation or stress induced side-effect stemming from the loss of GPL remains to be determined. It is clear that much remains to be learned regarding how *Mab* regulates the composition of its complex cell wall during infection and the roles of TCS like DosRS in host-pathogen interactions.

In addition to determination of the DosRS-dependent component of *Mab* hypoxia adaptation, this is the first transcriptomics study designed to identify genome-wide changes in *Mab* gene expression in a defined, physiologically relevant model of hypoxia. RNAseq analysis of wild-type *Mab*390S in 1% O_2 versus 20% O_2 identified an additional 1,063 DosRS-independent hypoxia-induced genes with putative roles in *Mab* adaptation in hypoxia. Differential gene expression of such a large group of genes in hypoxia outside of the DosR regulon points to a sophisticated mechanism of regulation for adaptation beyond TCS. This gene set included 80 TF, lipid metabolism and transport, energetics, secondary metabolism, cell wall synthesis plus induction of 540 hypothetical proteins, (Table S3). Our data highlights the necessity of adaptation to hypoxia *via* a large repertoire of genes including but not limited to the TCS DosRS. Further investigation of unique *Mab* DosR regulated genes and species-specific *Mab* genes employed for hypoxic adaptation will provide beneficial insights into *Mab* pathogenesis.

Data availability statement

The datasets presented in this study are deposited in the NCBI database, accession number PRJNA932814 (https://www.ncbi.nlm.nih.gov/bioproject/?term=PRJNA932814).

Author contributions

BS and KR: Conception and design of experiments. BS and BT: Analysis and interpretation of data for RNAseq experiments. BS and KR: Preparation and revision of manuscript. KR and LS: Approval of final manuscript. All authors contributed to the article and approved the submitted version.

Funding

LS acknowledges funding from the National Health Institute grant AI124458.

Acknowledgments

We would like to thank George Walters-Marrah for assistance with construction of luciferase reporter plasmids. We also thank Dr. Rushmi Gupta and Dr. Mollie Jewett for technical support and guidance.

Conflict of interest

The authors declare that the research was conducted in the absence of any commercial or financial relationships that could be construed as a potential conflict of interest.

Publisher's note

Supplementary material

The Supplementary Material for this article can be found online at: https://www.frontiersin.org/articles/10.3389/fcimb.2023.1144210/full#supplementary-material

References

Aguilar-Ayala, D. A., Tilleman, L., Van Nieuwerburgh, F., Deforce, D., Palomino, J. C., Vandamme, P., et al. (2017). The transcriptome of mycobacterium tuberculosis in a lipid-rich dormancy model through RNAseq analysis. *Sci. Rep.* 7 (1), 17665. doi: 10.1038/s41598-017-17751-x

Akhtar, S., Khan, A., Sohaskey, C. D., Jagannath, C., and Sarkar, D. (2013). Nitrite reductase NirBD is induced and plays an important role during *in vitro* dormancy of mycobacterium tuberculosis. *J. Bacteriol* 195 (20), 4592–4599. doi: 10.1128/JB.00698-13

Akusobi, C., Benghomari, B. S., Zhu, J., Wolf, I. D., Singhvi, S., Dulberger, C. L., et al. (2022). Transposon mutagenesis in mycobacterium abscessus identifies an essential penicillin-binding protein involved in septal peptidoglycan synthesis and antibiotic sensitivity. *Elife* 11. doi: 10.7554/eLife.71947.sa2

Amin, A. G., Goude, R., Shi, L., Zhang, J., Chatterjee, D., and Parish, T. (2008). EmbA is an essential arabinosyltransferase in mycobacterium tuberculosis. *Microbiol. (Reading)* 154 (Pt 1), 240–248. doi: 10.1099/mic.0.2007/012153-0

Andreu, N., Zelmer, A., Fletcher, T., Elkington, P. T., Ward, T. H., Ripoll, J., et al. (2010). Optimisation of bioluminescent reporters for use with mycobacteria. *PloS One* 5 (5), e10777. doi: 10.1371/journal.pone.0010777

Bacon, J., and Marsh, P. D. (2007). Transcriptional responses of mycobacterium tuberculosis exposed to adverse conditions *in vitro*. *Curr. Mol. Med.* 7 (3), 277–286. doi: 10.2174/156652407780598566

Bailo, R., Radhakrishnan, A., Singh, A., Nakaya, M., Fujiwara, N., and Bhatt, A. (2022). The mycobacterial desaturase DesA2 is associated with mycolic acid biosynthesis. *Sci. Rep.* 12 (1), 6943. doi: 10.1038/s41598-022-10589-y

Belardinelli, J. M., Verma, D., Li, W., Avanzi, C., Wiersma, C. J., Williams, J. T., et al. (2022). Therapeutic efficacy of antimalarial drugs targeting DosRS signaling in mycobacterium abscessus. *Sci. Transl. Med.* 14 (633), eabj3860. doi: 10.1126/scitranslmed.abj3860

Berney, M., and Cook, G. M. (2010). Unique flexibility in energy metabolism allows mycobacteria to combat starvation and hypoxia. *PloS One* 5 (1), e8614. doi: 10.1371/journal.pone.0008614

Bernut, A., Nguyen-Chi, M., Halloum, I., Herrmann, J. L., Lutfalla, G., and Kremer, L. (2016). Mycobacterium abscessus-induced granuloma formation is strictly dependent on TNF signaling and neutrophil trafficking. *PloS Pathog.* 12 (11), e1005986. doi: 10.1371/journal.ppat.1005986

Black, G. F., Thiel, B. A., Ota, M. O., Parida, S. K., Adegbola, R., Boom, W. H., et al. (2009). Immunogenicity of novel DosR regulon-encoded candidate antigens of mycobacterium tuberculosis in three high-burden populations in Africa. *Clin. Vaccine Immunol.* 16 (8), 1203–1212. doi: 10.1128/CVI.00111-09

Boldrin, F., Provvedi, R., Cioetto Mazzabo, L., Segafreddo, G., and Manganelli, R. (2020). Tolerance and persistence to drugs: A main challenge in the fight against mycobacterium tuberculosis. *Front. Microbiol.* 11, 1924. doi: 10.3389/fmicb.2020.01924

Bretl, D. J., Demetriadou, C., and Zahrt, T. C. (2011). Adaptation to environmental stimuli within the host: Two-component signal transduction systems of mycobacterium tuberculosis. *Microbiol. Mol. Biol. Rev.* 75 (4), 566–582. doi: 10.1128/MMBR.05004-11

Brown-Elliott, B. A., and Wallace, R. J.Jr. (2002). Clinical and taxonomic status of pathogenic nonpigmented or late-pigmenting rapidly growing mycobacteria. *Clin. Microbiol. Rev.* 15 (4), 716–746. doi: 10.1128/CMR.15.4.716-746.2002

Byrd, T. F., and Lyons, C. R. (1999). Preliminary characterization of a mycobacterium abscessus mutant in human and murine models of infection. *Infect. Immun.* 67 (9), 4700–4707. doi: 10.1128/IAI.67.9.4700-4707.1999

Capyk, J. K., Kalscheuer, R., Stewart, G. R., Liu, J., Kwon, H., Zhao, R., et al. (2009). Mycobacterial cytochrome p450 125 (cyp125) catalyzes the terminal hydroxylation of c27 steroids. *J. Biol. Chem.* 284 (51), 35534–35542. doi: 10.1074/jbc.M109.072132

Catherinot, E., Roux, A. L., Macheras, E., Hubert, D., Matmar, M., Dannhoffer, L., et al. (2009). Acute respiratory failure involving an r variant of mycobacterium abscessus. *J. Clin. Microbiol.* 47 (1), 271–274. doi: 10.1128/JCM.01478-08

Chmiel, J. F., and Davis, P. B. (2003). State of the art: Why do the lungs of patients with cystic fibrosis become infected and why can't they clear the infection? *Respir. Res.* 4, 8. doi: 10.1186/1465-9921-4-8

Converse, P. J., Karakousis, P. C., Klinkenberg, L. G., Kesavan, A. K., Ly, L. H., Allen, S. S., et al. (2009). Role of the dosR-dosS two-component regulatory system in mycobacterium tuberculosis virulence in three animal models. *Infect. Immun.* 77 (3), 1230–1237. doi: 10.1128/IAI.01117-08

Cook, G. M., Hards, K., Vilcheze, C., Hartman, T., and Berney, M. (2014). Energetics of respiration and oxidative phosphorylation in mycobacteria. *Microbiol. Spectr.* 2 (3). doi: 10.1128/9781555818845.ch20

Cunningham, A. F., and Spreadbury, C. L. (1998). Mycobacterial stationary phase induced by low oxygen tension: Cell wall thickening and localization of the 16-kilodalton alpha-crystallin homolog. *J. Bacteriol* 180 (4), 801–808. doi: 10.1128/JB.180.4.801-808.1998

Cunningham-Bussel, A., Zhang, T., and Nathan, C. F. (2013). Nitrite produced by mycobacterium tuberculosis in human macrophages in physiologic oxygen impacts bacterial ATP consumption and gene expression. *Proc. Natl. Acad. Sci. U.S.A.* 110 (45), E4256–E4265. doi: 10.1073/pnas.1316894110

Daher, W., Leclercq, L. D., Johansen, M. D., Hamela, C., Karam, J., Trivelli, X., et al. (2022). Glycopeptidolipid glycosylation controls surface properties and pathogenicity in mycobacterium abscessus. *Cell Chem. Biol.* 29 (5), 910–924 e917. doi: 10.1016/j.chembiol.2022.03.008

Daniel, J., Deb, C., Dubey, V. S., Sirakova, T. D., Abomoelak, B., Morbidoni, H. R., et al. (2004). Induction of a novel class of diacylglycerol acyltransferases and triacylglycerol accumulation in mycobacterium tuberculosis as it goes into a dormancy-like state in culture. *J. Bacteriol* 186 (15), 5017–5030. doi: 10.1128/JB.186.15.5017-5030.2004

Deb, C., Lee, C. M., Dubey, V. S., Daniel, J., Abomoelak, B., Sirakova, T. D., et al. (2009). A novel *in vitro* multiple-stress dormancy model for mycobacterium tuberculosis generates a lipid-loaded, drug-tolerant, dormant pathogen. *PloS One* 4 (6), e6077. doi: 10.1371/journal.pone.0006077

Dubois, V., Pawlik, A., Bories, A., Le Moigne, V., Sismeiro, O., Legendre, R., et al. (2019). Mycobacterium abscessus virulence traits unraveled by transcriptomic profiling in amoeba and macrophages. *PloS Pathog.* 15 (11), e1008069. doi: 10.1371/journal.ppat.1008069

Esther, C. R.Jr., Esserman, D. A., Gilligan, P., Kerr, A., and Noone, P. G. (2010). Chronic mycobacterium abscessus infection and lung function decline in cystic fibrosis. *J. Cyst Fibros* 9 (2), 117–123. doi: 10.1016/j.jcf.2009.12.001

Fol, M., Chauhan, A., Nair, N. K., Maloney, E., Moomey, M., Jagannath, C., et al. (2006). Modulation of mycobacterium tuberculosis proliferation by MtrA, an essential two-component response regulator. *Mol. Microbiol.* 60 (3), 643–657. doi: 10.1111/j.1365-2958.2006.05137.x

Galagan, J. E., Minch, K., Peterson, M., Lyubetskaya, A., Azizi, E., Sweet, L., et al. (2013). The mycobacterium tuberculosis regulatory network and hypoxia. *Nature* 499 (7457), 178–183. doi: 10.1038/nature12337

Garton, N. J., Waddell, S. J., Sherratt, A. L., Lee, S. M., Smith, R. J., Senner, C., et al. (2008). Cytological and transcript analyses reveal fat and lazy persister-like bacilli in tuberculous sputum. *PloS Med.* 5 (4), e75. doi: 10.1371/journal.pmed.0050075

Gautam, U. S., McGillivray, A., Mehra, S., Didier, P. J., Midkiff, C. C., Kissee, R. S., et al. (2015a). DosS is required for the complete virulence of mycobacterium tuberculosis in mice with classical granulomatous lesions. *Am. J. Respir. Cell Mol. Biol.* 52 (6), 708–716. doi: 10.1165/rcmb.2014-0230OC

Gautam, U. S., Mehra, S., and Kaushal, D. (2015b). In-vivo gene signatures of mycobacterium tuberculosis in C3HeB/FeJ mice. *PloS One* 10 (8), e0135208. doi: 10.1371/journal.pone.0135208

Gautam, U. S., Mehra, S., Kumari, P., Alvarez, X., Niu, T., Tyagi, J. S., et al. (2019). Mycobacterium tuberculosis sensor kinase DosS modulates the autophagosome in a DosR-independent manner. *Commun. Biol.* 2, 349. doi: 10.1038/s42003-019-0594-0

Gerasimova, A., Kazakov, A. E., Arkin, A. P., Dubchak, I., and Gelfand, M. S. (2011). Comparative genomics of the dormancy regulons in mycobacteria. *J. Bacteriol* 193 (14), 3446–3452. doi: 10.1128/JB.00179-11

Gold, B., and Nathan, C. (2017). Targeting phenotypically tolerant mycobacterium tuberculosis. *Microbiol. Spectr.* 5 (1). doi: 10.1128/microbiolspec.TBTB2-0031-2016

Gonzalo-Asensio, J., Mostowy, S., Harders-Westerveen, J., Huygen, K., Hernandez-Pando, R., Thole, J., et al. (2008). PhoP: A missing piece in the intricate puzzle of mycobacterium tuberculosis virulence. *PloS One* 3 (10), e3496. doi: 10.1371/journal.pone.0003496

Gooderham, W. J., and Hancock, R. E. (2009). Regulation of virulence and antibiotic resistance by two-component regulatory systems in pseudomonas aeruginosa. *FEMS Microbiol. Rev.* 33 (2), 279–294. doi: 10.1111/j.1574-6976.2008.00135.x

Greendyke, R., and Byrd, T. F. (2008). Differential antibiotic susceptibility of mycobacterium abscessus variants in biofilms and macrophages compared to that of planktonic bacteria. *Antimicrob. Agents Chemother.* 52 (6), 2019–2026. doi: 10.1128/AAC.00986-07

Gutierrez, A. V., Baron, S. A., Sardi, F. S., Saad, J., Coltey, B., Reynaud-Gaubert, M., et al. (2021). Beyond phenotype: The genomic heterogeneity of co-infecting mycobacterium abscessus smooth and rough colony variants in cystic fibrosis patients. *J. Cyst Fibros* 20 (3), 421–423. doi: 10.1016/j.jcf.2021.02.002

Gutierrez, A. V., Viljoen, A., Ghigo, E., Herrmann, J. L., and Kremer, L. (2018). Glycopeptidolipids, a double-edged sword of the mycobacterium abscessus complex. *Front. Microbiol.* 9, 1145. doi: 10.3389/fmicb.2018.01145

Harris, K. A., and Kenna, D. T. (2014). Mycobacterium abscessus infection in cystic fibrosis: molecular typing and clinical outcomes. *J. Med. Microbiol.* 63 (Pt 10), 1241–1246. doi: 10.1099/jmm.0.077164-0

Honaker, R. W., Leistikow, R. L., Bartek, I. L., and Voskuil, M. I. (2009). Unique roles of DosT and DosS in DosR regulon induction and mycobacterium tuberculosis dormancy. *Infect. Immun.* 77 (8), 3258–3263. doi: 10.1128/IAI.01449-08

Hudock, T. A., Foreman, T. W., Bandyopadhyay, N., Gautam, U. S., Veatch, A. V., LoBato, D. N., et al. (2017). Hypoxia sensing and persistence genes are expressed during the intragranulomatous survival of mycobacterium tuberculosis. *Am. J. Respir. Cell Mol. Biol.* 56 (5), 637–647. doi: 10.1165/rcmb.2016-0239OC

Hurst-Hess, K., Rudra, P., and Ghosh, P. (2017). Mycobacterium abscessus WhiB7 regulates a species-specific repertoire of genes to confer extreme antibiotic resistance. *Antimicrob. Agents Chemother.* 61 (11). doi: 10.1128/AAC.01347-17

Jonsson, B. E., Gilljam, M., Lindblad, A., Ridell, M., Wold, A. E., and Welinder-Olsson, C. (2007). Molecular epidemiology of mycobacterium abscessus, with focus on cystic fibrosis. *J. Clin. Microbiol.* 45 (5), 1497–1504. doi: 10.1128/JCM.02592-06

Joshi, H., Kandari, D., and Bhatnagar, R. (2021). Insights into the molecular determinants involved in mycobacterium tuberculosis persistence and their therapeutic implications. *Virulence* 12 (1), 2721–2749. doi: 10.1080/21505594.2021.1990660

Kendall, S. L., Movahedzadeh, F., Rison, S. C., Wernisch, L., Parish, T., Duncan, K., et al. (2004). The mycobacterium tuberculosis dosRS two-component system is induced by multiple stresses. *Tuberculosis (Edinb)* 84 (3-4), 247–255. doi: 10.1016/j.tube.2003.12.007

Kester, J. C., Kandror, O., Akopian, T., Chase, M. R., Zhu, J., Rubin, E. J., et al. (2021). ClpX is essential and activated by single-strand DNA binding protein in mycobacteria. *J. Bacteriol* 203 (4). doi: 10.1128/JB.00608-20

Klepp, L. I., Sabio, Y. G. J., and FabianaBigi, (2022). Mycobacterial MCE proteins as transporters that control lipid homeostasis of the cell wall. *Tuberculosis (Edinb)* 132, 102162. doi: 10.1016/j.tube.2021.102162

Kundu, M., and Basu, J. (2021). Applications of transcriptomics and proteomics for understanding dormancy and resuscitation in mycobacterium tuberculosis. *Front. Microbiol.* 12, 642487. doi: 10.3389/fmicb.2021.642487

Lee, M. R., Sheng, W. H., Hung, C. C., Yu, C. J., Lee, L. N., and Hsueh, P. R. (2015). Mycobacterium abscessus complex infections in humans. *Emerg. Infect. Dis.* 21 (9), 1638–1646. doi: 10.1126/scitranslmed.abj3860

Leistikow, R. L., Morton, R. A., Bartek, I. L., Frimpong, I., Wagner, K., and Voskuil, M. I. (2010). The mycobacterium tuberculosis DosR regulon assists in metabolic homeostasis and enables rapid recovery from nonrespiring dormancy. *J. Bacteriol* 192 (6), 1662–1670. doi: 10.1128/JB.00926-09

Li, X., Lv, X., Lin, Y., Zhen, J., Ruan, C., Duan, W., et al. (2019). Role of two-component regulatory systems in intracellular survival of mycobacterium tuberculosis. *J. Cell Biochem.* 120 (8), 12197–12207. doi: 10.1002/jcb.28792

Li, C., Wen, A., Shen, B., Lu, J., Huang, Y., and Chang, Y. (2011). FastCloning: a highly simplified, purification-free, sequence- and ligation-independent PCR cloning method. *BMC Biotechnol.* 11, 92. doi: 10.1186/1472-6750-11-92

Li, B., Ye, M., Zhao, L., Guo, Q., Chen, J., Xu, B., et al. (2020). Glycopeptidolipid genotype correlates with the severity of mycobacterium abscessus lung disease. *J. Infect. Dis.* 221 (Suppl 2), S257–S262. doi: 10.1093/infdis/jiz475

Lin, M. Y., Reddy, T. B., Arend, S. M., Friggen, A. H., Franken, K. L., van Meijgaarden, K. E., et al. (2009). Cross-reactive immunity to mycobacterium tuberculosis DosR regulon-encoded antigens in individuals infected with environmental, nontuberculous mycobacteria. *Infect. Immun.* 77 (11), 5071–5079. doi: 10.1128/IAI.00457-09

Lopeman, R. C., Harrison, J., Desai, M., and Cox, J. A. G. (2019). Mycobacterium abscessus: Environmental bacterium turned clinical nightmare. *Microorganisms* 7 (3). doi: 10.3390/microorganisms7030090

Lyczak, J. B., Cannon, C. L., and Pier, G. B. (2002). Lung infections associated with cystic fibrosis. *Clin. Microbiol. Rev.* 15 (2), 194–222. doi: 10.1128/CMR.15.2.194-222.2002

Madacki, J., Laval, F., Grzegorzewicz, A., Lemassu, A., Zahorszka, M., Arand, M., et al. (2018). Impact of the epoxide hydrolase EphD on the metabolism of mycolic acids in mycobacteria. *J. Biol. Chem.* 293 (14), 5172–5184. doi: 10.1074/jbc.RA117.000246

Malhotra, V., Agrawal, R., Duncan, T. R., Saini, D. K., and Clark-Curtiss, J. E. (2015). Mycobacterium tuberculosis response regulators, DevR and NarL, interact *in vivo* and co-regulate gene expression during aerobic nitrate metabolism. *J. Biol. Chem.* 290 (13), 8294–8309. doi: 10.1074/jbc.M114.591800

Malhotra, S., Vedithi, S. C., and Blundell, T. L. (2017). Decoding the similarities and differences among mycobacterial species. *PloS Negl. Trop. Dis.* 11 (8), e0005883. doi: 10.1371/journal.pntd.0005883

Malm, S., Tiffert, Y., Micklinghoff, J., Schultze, S., Joost, I., Weber, I., et al. (2009). The roles of the nitrate reductase NarGHJI, the nitrite reductase NirBD and the response regulator GlnR in nitrate assimilation of mycobacterium tuberculosis. *Microbiol. (Reading)* 155 (Pt 4), 1332–1339. doi: 10.1099/mic.0.023275-0

Mascher, T., Helmann, J. D., and Unden, G. (2006). Stimulus perception in bacterial signal-transducing histidine kinases. *Microbiol. Mol. Biol. Rev.* 70 (4), 910–938. doi: 10.1128/MMBR.00020-06

Mehra, S., Foreman, T. W., Didier, P. J., Ahsan, M. H., Hudock, T. A., Kissee, R., et al. (2015). The DosR regulon modulates adaptive immunity and is essential for mycobacterium tuberculosis persistence. *Am. J. Respir. Crit. Care Med.* 191 (10), 1185–1196. doi: 10.1164/rccm.201408-1502OC

Miranda-CasoLuengo, A. A., Staunton, P. M., Dinan, A. M., Lohan, A. J., and Loftus, B. J. (2016). Functional characterization of the mycobacterium abscessus genome coupled with condition specific transcriptomics reveals conserved molecular strategies for host adaptation and persistence. *BMC Genomics* 17, 553. doi: 10.1186/s12864-016-2868-y

Molina-Torres, C. A., Tamez-Pena, L., Castro-Garza, J., Ocampo-Candiani, J., and Vera-Cabrera, L. (2018). Evaluation of the intracellular activity of drugs against mycobacterium abscessus using a THP-1 macrophage model. *J. Microbiol. Methods* 148, 29–32. doi: 10.1016/j.mimet.2018.03.020

Moore, S. D., and Prevelige, P. E.Jr. (2002). A P22 scaffold protein mutation increases the robustness of head assembly in the presence of excess portal protein. *J. Virol.* 76 (20), 10245–10255. doi: 10.1128/JVI.76.20.10245-10255.2002

Nessar, R., Cambau, E., Reyrat, J. M., Murray, A., and Gicquel, B. (2012). Mycobacterium abscessus: A new antibiotic nightmare. *J. Antimicrob. Chemother.* 67 (4), 810–818. doi: 10.1093/jac/dkr578

Olivier, K. N., Weber, D. J., Wallace, R. J.Jr., Faiz, A. R., Lee, J. H., Zhang, Y., et al. (2003). Nontuberculous mycobacteria. I: Multicenter prevalence study in cystic fibrosis. *Am. J. Respir. Crit. Care Med.* 167 (6), 828–834. doi: 10.1164/rccm.200207-678OC

Ortega Ugalde, S., Boot, M., Commandeur, J. N. M., Jennings, P., Bitter, W., and Vos, J. C. (2019). Function, essentiality, and expression of cytochrome P450 enzymes and their cognate redox partners in mycobacterium tuberculosis: Are they drug targets? *Appl. Microbiol. Biotechnol.* 103 (9), 3597–3614. doi: 10.1007/s00253-019-09697-z

Park, H. D., Guinn, K. M., Harrell, M. I., Liao, R., Voskuil, M. I., Tompa, M., et al. (2003). Rv3133c/dosR is a transcription factor that mediates the hypoxic response of mycobacterium tuberculosis. *Mol. Microbiol.* 48 (3), 833–843. doi: 10.1046/j.1365-2958.2003.03474.x

Pawlik, A., Garnier, G., Orgeur, M., Tong, P., Lohan, A., Le Chevalier, F., et al. (2013). Identification and characterization of the genetic changes responsible for the characteristic smooth-to-rough morphotype alterations of clinically persistent mycobacterium abscessus. *Mol. Microbiol.* 90 (3), 612–629. doi: 10.1111/mmi.12387

Peddireddy, V., Doddam, S. N., and Ahmed, N. (2017). Mycobacterial dormancy systems and host responses in tuberculosis. *Front. Immunol.* 8, 84. doi: 10.3389/fimmu.2017.00084

Peterson, E. J. R., Abidi, A. A., Arrieta-Ortiz, M. L., Aguilar, B., Yurkovich, J. T., Kaur, A., et al. (2020). Intricate genetic programs controlling dormancy in mycobacterium tuberculosis. *Cell Rep.* 31 (4), 107577. doi: 10.1016/j.celrep.2020.107577

Philley, J. V., DeGroote, M. A., Honda, J. R., Chan, M. M., Kasperbauer, S., Walter, N. D., et al. (2016). Treatment of non-tuberculous mycobacterial lung disease. *Curr. Treat Options Infect. Dis.* 8 (4), 275–296. doi: 10.1007/s40506-016-0086-4

Plocinska, R., Wasik, K., Plocinski, P., Lechowicz, E., Antczak, M., Blaszczyk, E., et al. (2022). The orphan response regulator Rv3143 modulates the activity of the NADH dehydrogenase complex (Nuo) in mycobacterium tuberculosis *via* protein-protein interactions. *Front. Cell Infect. Microbiol.* 12, 909507. doi: 10.3389/fcimb.2022.909507

Purkayastha, A., McCue, L. A., and McDonough, K. A. (2002). Identification of a mycobacterium tuberculosis putative classical nitroreductase gene whose expression is coregulated with that of the acr aene within macrophages, in standing versus shaking cultures, and under low oxygen conditions. *Infect. Immun.* 70 (3), 1518–1529. doi: 10.1128/IAI.70.3.1518-1529.2002

Rathor, N., Garima, K., Sharma, N. K., Narang, A., Varma-Basil, M., and Bose, M. (2016). Expression profile of mce4 operon of mycobacterium tuberculosis following environmental stress. *Int. J. Mycobacteriol* 5 (3), 328–332. doi: 10.1016/j.ijmyco.2016.08.004

Roberts, D. M., Liao, R. P., Wisedchaisri, G., Hol, W. G., and Sherman, D. R. (2004). Two sensor kinases contribute to the hypoxic response of mycobacterium tuberculosis. *J. Biol. Chem.* 279 (22), 23082–23087. doi: 10.1074/jbc.M401230200

Rohde, K. H., Abramovitch, R. B., and Russell, D. G. (2007). Mycobacterium tuberculosis invasion of macrophages: linking bacterial gene expression to environmental cues. *Cell Host Microbe* 2 (5), 352–364. doi: 10.1016/j.chom.2007.09.006

Rohde, K. H., Veiga, D. F., Caldwell, S., Balazsi, G., and Russell, D. G. (2012). Linking the transcriptional profiles and the physiological states of mycobacterium tuberculosis during an extended intracellular infection. *PloS Pathog.* 8 (6), e1002769. doi: 10.1371/journal.ppat.1002769

Roux, A. L., Viljoen, A., Bah, A., Simeone, R., Bernut, A., Laencina, L., et al. (2016). The distinct fate of smooth and rough mycobacterium abscessus variants inside macrophages. *Open Biol.* 6 (11). doi: 10.1098/rsob.160185

Ruger, K., Hampel, A., Billig, S., Rucker, N., Suerbaum, S., and Bange, F. C. (2014). Characterization of rough and smooth morphotypes of mycobacterium abscessus isolates from clinical specimens. *J. Clin. Microbiol.* 52 (1), 244–250. doi: 10.1128/JCM.01249-13

Rustad, T. R., Harrell, M. I., Liao, R., and Sherman, D. R. (2008). The enduring hypoxic response of mycobacterium tuberculosis. *PloS One* 3 (1), e1502. doi: 10.1371/journal.pone.0001502

Rustad, T. R., Sherrid, A. M., Minch, K. J., and Sherman, D. R. (2009). Hypoxia: a window into mycobacterium tuberculosis latency. *Cell Microbiol.* 11 (8), 1151–1159. doi: 10.1111/j.1462-5822.2009.01325.x

Salazar, M. E., and Laub, M. T. (2015). Temporal and evolutionary dynamics of two-component signaling pathways. *Curr. Opin. Microbiol.* 24, 7–14. doi: 10.1016/j.mib.2014.12.003

Santangelo Mde, L., Blanco, F., Campos, E., Soria, M., Bianco, M. V., Klepp, L., et al. (2009). Mce2R from mycobacterium tuberculosis represses the expression of the mce2 operon. *Tuberculosis (Edinb)* 89 (1), 22–28. doi: 10.1016/j.tube.2008.09.002

Sassetti, C. M., Boyd, D. H., and Rubin, E. J. (2003). Genes required for mycobacterial growth defined by high density mutagenesis. *Mol. Microbiol.* 48 (1), 77–84. doi: 10.1046/j.1365-2958.2003.03425.x

Sherman, D. R., Voskuil, M., Schnappinger, D., Liao, R., Harrell, M. I., and Schoolnik, G. K. (2001). Regulation of the mycobacterium tuberculosis hypoxic response gene encoding alpha -crystallin 98, 13, 7534–7539. doi: 10.1073/pnas.121172498

Singh, A., Mai, D., Kumar, A., and Steyn, A. J. (2006). Dissecting virulence pathways of mycobacterium tuberculosis through protein-protein association. *Proc. Natl. Acad. Sci. U.S.A.* 103 (30), 11346–11351. doi: 10.1073/pnas.0602817103

Singh, A., Varela, C., Bhatt, K., Veerapen, N., Lee, O. Y., Wu, H. H., et al. (2016). Identification of a desaturase involved in mycolic acid biosynthesis in mycobacterium smegmatis. *PloS One* 11 (10), e0164253. doi: 10.1371/journal.pone.0164253

Stock, J. B., Ninfa, A. J., and Stock, A. M. (1989). Protein phosphorylation and regulation of adaptive responses in bacteria. *Microbiol. Rev.* 53 (4), 450–490. doi: 10.1128/mr.53.4.450-490.1989

Story-Roller, E., Maggioncalda, E. C., Cohen, K. A., and Lamichhane, G. (2018). Mycobacterium abscessus and beta-lactams: Emerging insights and potential opportunities. *Front. Microbiol.* 9, 2273. doi: 10.3389/fmicb.2018.02273

Stupar, M., Furness, J., De Voss, C. J., Tan, L., and West, N. P. (2022). Two-component sensor histidine kinases of mycobacterium tuberculosis: Beacons for niche navigation. *Mol. Microbiol.* 117 (5), 973–985. doi: 10.1111/mmi.14899

Tomlinson, B. R., Denham, G. A., Torres, N. J., Brzozowski, R. S., Allen, J. L., Jackson, J. K., et al. (2022). Assessing the role of cold-shock protein c: a novel regulator of acinetobacter baumannii biofilm formation and virulence. *Infect. Immun.* 90 (10), e0037622. doi: 10.1128/iai.00376-22

Tomlinson, B. R., Malof, M. E., and Shaw, L. N. (2021). A global transcriptomic analysis of staphylococcus aureus biofilm formation across diverse clonal lineages. *Microb. Genom* 7 (7). doi: 10.1099/mgen.0.000598

Tsai, S. H., Lai, H. C., and Hu, S. T. (2015). Subinhibitory doses of aminoglycoside antibiotics induce changes in the phenotype of mycobacterium abscessus. *Antimicrob. Agents Chemother.* 59 (10), 6161–6169. doi: 10.1128/AAC.01132-15

Unden, G., and Bongaerts, J. (1997). Alternative respiratory pathways of escherichia coli: Energetics and transcriptional regulation in response to electron acceptors. *Biochim. Biophys. Acta* 1320 (3), 217–234. doi: 10.1016/S0005-2728(97)00034-0

van Kessel, J. C., and Hatfull, G. F. (2007). Recombineering in mycobacterium tuberculosis. *Nat. Methods* 4 (2), 147–152. doi: 10.1038/nmeth996

Veatch, A. V., and Kaushal, D. (2018). Opening pandora's box: Mechanisms of mycobacterium tuberculosis resuscitation. *Trends Microbiol.* 26 (2), 145–157. doi: 10.1016/j.tim.2017.08.001

Vilcheze, C., Yan, B., Casey, R., Hingley-Wilson, S., Ettwiller, L., and Jacobs, W. R.Jr. (2022). Commonalities of mycobacterium tuberculosis transcriptomes in response to defined persisting macrophage stresses. *Front. Immunol.* 13, 909904. doi: 10.3389/fimmu.2022.909904

Viljoen, A., Blaise, M., de Chastellier, C., and Kremer, L. (2016). MAB_3551c encodes the primary triacylglycerol synthase involved in lipid accumulation in mycobacterium abscessus. *Mol. Microbiol.* 102 (4), 611–627. doi: 10.1111/mmi.13482

Voskuil, M. I., Schnappinger, D., Visconti, K. C., Harrell, M. I., Dolganov, G. M., Sherman, D. R., et al. (2003). Inhibition of respiration by nitric oxide induces a mycobacterium tuberculosis dormancy program. *J. Exp. Med.* 198 (5), 705–713. doi: 10.1084/jem.20030205

Voskuil, M. I., Visconti, K. C., and Schoolnik, G. K. (2004). Mycobacterium tuberculosis gene expression during adaptation to stationary phase and low-oxygen dormancy. *Tuberculosis (Edinb)* 84 (3-4), 218–227. doi: 10.1016/j.tube.2004.02.003

Walters, S. B., Dubnau, E., Kolesnikova, I., Laval, F., Daffe, M., and Smith, I. (2006). The mycobacterium tuberculosis PhoPR two-component system regulates genes essential for virulence and complex lipid biosynthesis. *Mol. Microbiol.* 60 (2), 312–330. doi: 10.1111/j.1365-2958.2006.05102.x

Wee, W. Y., Dutta, A., and Choo, S. W. (2017). Comparative genome analyses of mycobacteria give better insights into their evolution. *PloS One* 12 (3), e0172831. doi: 10.1371/journal.pone.0172831

Weinstein, E. A., Yano, T., Li, L. S., Avarbock, D., Avarbock, A., Helm, D., et al. (2005). Inhibitors of type II NADH:menaquinone oxidoreductase represent a class of antitubercular drugs. *Proc. Natl. Acad. Sci. U.S.A.* 102 (12), 4548–4553. doi: 10.1073/pnas.0500469102

West, A. H., and Stock, A. M. (2001). Histidine kinases and response regulator proteins in two-component signaling systems. *Trends Biochem. Sci.* 26 (6), 369–376. doi: 10.1016/S0968-0004(01)01852-7

Wilburn, K. M., Fieweger, R. A., and VanderVen, B. C. (2018). Cholesterol and fatty acids grease the wheels of mycobacterium tuberculosis pathogenesis. *Pathog. Dis.* 76 (2). doi: 10.1093/femspd/fty021

Worlitzsch, D., Tarran, R., Ulrich, M., Schwab, U., Cekici, A., Meyer, K. C., et al. (2002). Effects of reduced mucus oxygen concentration in airway pseudomonas infections of cystic fibrosis patients. *J. Clin. Invest.* 109 (3), 317–325. doi: 10.1172/JCI0213870

Yang, H., Wang, F., Guo, X., Liu, F., Liu, Z., Wu, X., et al. (2021). Interception of host fatty acid metabolism by mycobacteria under hypoxia to suppress anti-TB immunity. *Cell Discovery* 7 (1), 90. doi: 10.1038/s41421-021-00301-1

Yarwood, J. M., McCormick, J. K., and Schlievert, P. M. (2001). Identification of a novel two-component regulatory system that acts in global regulation of virulence

factors of staphylococcus aureus. *J. Bacteriol* 183 (4), 1113–1123. doi: 10.1128/JB.183.4.1113-1123.2001

Yeruva, V. C., Savanagouder, M., Khandelwal, R., Kulkarni, A., Sharma, Y., and Raghunand, T. R. (2016). The mycobacterium tuberculosis desaturase DesA1 (Rv0824c) is a Ca(2+) binding protein. *Biochem. Biophys. Res. Commun.* 480 (1), 29–35. doi: 10.1016/j.bbrc.2016.10.014

Yousuf, S., Angara, R. K., Roy, A., Gupta, S. K., Misra, R., and Ranjan, A. (2018). Mce2R/Rv0586 of mycobacterium tuberculosis is the functional homologue of FadR(E. coli). *Microbiol. (Reading)* 164 (9), 1133–1145. doi: 10.1099/mic.0.000686

Zhu, C., Liu, Y., Hu, L., Yang, M., and He, Z. G. (2018). Molecular mechanism of the synergistic activity of ethambutol and isoniazid against mycobacterium tuberculosis. *J. Biol. Chem.* 293 (43), 16741–16750. doi: 10.1074/jbc.RA118.002693